ÇUKUROVA UNIVERSITY

INSTITUTE OF NATURAL AND APPLIED SCIENCES

MSc THESIS

Investigation of Mechanical Behaviors of Additively Manufactured Inconel 718 Superalloys Used in Aerospace Applications

Can DOĞAN

Mechanical Engineering Department

February, 2024

ÇUKUROVA UNIVERSITY

INSTITUTE OF NATURAL AND APPLIED SCIENCES

MSc THESIS APPROVAL

Investigation of Mechanical Behaviors of Additively Manufactured Inconel 718 Superalloys Used in Aerospace Applications

Can DOĞAN

Mechanical Engineering Department

This Master's Thesis was evaluated by the following Jury Members on 21/ 02/ 2024 and was approved by unanimity / majority of votes.

Jury : Asst. Prof. Dr. Durmuş Ali BİRCAN (Advisor) ……

: Assoc. Prof. Dr. Mehmet İlteriş SARIGEÇİLİ ……

: Assoc. Prof. Dr. Erinç ULUDAMAR ……

This Thesis was written in the Department of Mechanical Engineering, Institute of Natural and Applied Sciences.
Thesis Number:

Prof. Dr. Sadık DİNÇER
Director
Institute of Natural and Applied Sciences

Note: The usage of the presented specific declarations, tables, figures, and photographs either in this thesis or in any other reference without citation is subject to "The law of Arts and Intellectual Products" number of 5846 of Turkish Republic

CONTENTS

ABSTRACT I
ÖZ II
EXTENDED ABSTRACT III
GENİŞLETİLMİŞ ÖZET VI
ACKNOWLEDGEMENTS IX
LIST OF TABLES X
LIST OF FIGURES XI
SYMBOLS AND ABBREVIATIONS XIII
1. INTRODUCTION 1
1.1. Overview of Superalloys and Applications 1
1.2. Mechanical Behavior of Inconel 718 4
1.3. Importance in Aerospace, Automotive, Nuclear, and Petrochemical Industries 6
1.4. Manufacturing Methods and Their Limitations for Complex Geometries 7
1.5. The Need for Net Shape Production 8
1.6. Introduction to Additive Manufacturing and SLM 8
1.7. The Effect of Post Heat Treating on the Mechanical Characteristics 12
2. LITERATURE REVIEW 15
3. MATERIALS AND METHODS 21
3.1. Material 21
3.2. Production of the Samples 23
3.3. Effects of Manufacturing Direction 24
3.4. Heat Treatment Procedures 25
3.5. Mechanical Tests 27
3.5.1. XRF Analysis 27
3.5.2. Tensile Testing 28
3.5.3. Hardness Measurements 29
4. RESULTS AND DISCUSSION 31
4.1. XRF Analysis 31
4.2. Tensile Tests 32
4.2.1. Horizontal Production Direction 32
4.2.2. Vertical Production Direction 35
4.3. Evaluation of Hardness Measurements 38
4.3.1. The Impact of Post Heat Treatments on the Mechanical Characteristics 44
5. CONCLUSION AND FUTURE STUDIES 49

5.1. Conclusion 49
5.2. Future Studies 51
REFERENCES 53
CURRICULUM VITAE 59

CUKUROVA UNIVERSITY

INSTITUTE OF NATURAL AND APPLIED SCIENCES

MSc THESIS

Investigation of Mechanical Behaviors of Additively Manufactured Inconel 718 Superalloys Used in Aerospace Applications

Can DOĞAN

Advisor: Asist. Prof. Dr. Durmuş Ali BİRCAN

Department of Mechanical Engineering

ABSTRACT

Inconel 718 (IN718) is a nickel-based superalloy widely used in a variety of high temperature applications due to its outstanding mechanical properties and resistance to environmental degradation. It exhibits high strength, excellent fatigue and creep resistance, oxidation resistance and favorable weldability at elevated temperatures. IN718 has traditionally been produced and applied through forging, casting, and powder metallurgy. However, Additive Manufacturing (AM) is a new processing method that is gaining popularity in the aerospace, automotive, and defense industries. AM enables the production of complex geometries with high material utilization and shorter lead times compared to traditional methods. Among the various AM techniques, Selective Laser Melting (SLM) has shown potential for near net shape production of Ni based high temperature components, including IN718. SLM is a highly flexible and customizable AM technique, making it well suited for the production of complex critical parts, for example aero engine components. SLM uses a focused laser beam to selectively melt and fuse metal powders layer by layer according to a Three-Dimensional (3D) Computer Aided Design (CAD) model. However, parts produced using SLM often exhibit certain microstructural defects that can compromise their mechanical properties. These include residual stresses, porosity and microstructural defects such as grain boundaries and precipitates. To overcome these defects and improve the mechanical properties of SLM-produced (SLMed) IN718, post-heat treatment processes are used. This study examines the mechanical behaviour (tensile and hardness) of SLMed IN718 parts, taking into account the direction of fabrication and the heat treatments applied, including homogenization annealing and new aging. The findings offer valuable information for improving the fabrication process and achieving the desired mechanical properties in high-temperature components. Combining AM techniques with appropriate heat treatments has great potential for producing net-shape IN718 parts with complex geometries for high-performance requirements.

Keywords: Inconel 718, Superalloy, Additive Manufacturing, Aerospace, Selective Laser Melting.

ÇUKUROVA ÜNİVERSİTESİ
FEN BİLİMLERİ ENSTİTÜSÜ

YÜKSEK LİSANS TEZİ

Havacılık ve Uzay Uygulamalarında Kullanılan Eklemeli İmalat ile Üretilen Inconel 718 Süper Alaşımlarının Mekanik Davranışlarının İncelenmesi

Can DOĞAN

Danışman: Asist. Prof. Dr. Durmuş Ali BİRCAN

Makine Mühendisliği Anabilim Dalı

ÖZ

Inconel 718 (IN718), üstün mekanik özellikleri ve çevresel bozulmaya karşı direnci nedeniyle çeşitli yüksek sıcaklık uygulamalarında yaygın olarak kullanılan nikel bazlı bir süper alaşımdır. Yüksek mukavemet, mükemmel yorulma ve sürünme direnci, oksidasyon direnci ve yüksek sıcaklıklarda uygun kaynaklanabilirlik sergiler. IN718 geleneksel olarak dövme, döküm ve toz metalurjisi yoluyla üretilmiş ve uygulanmıştır. Ancak, Katmanlı Üretim (AM) havacılık, otomotiv ve savunma sanayilerinde popülerlik kazanan yeni bir işleme yöntemidir. AM, geleneksel yöntemlere kıyasla yüksek malzeme faydalanımı ve daha kısa üretim süreleri ile karmaşık geometrilerin üretilmesini sağlar. Çeşitli AM teknikleri arasında Seçici Lazer Eritme (SLM), IN718 de dahil olmak üzere Ni bazlı yüksek sıcaklık bileşenlerinin net şekle yakın üretimi için potansiyel göstermektedir. SLM son derece esnek ve özelleştirilebilir bir AM tekniğidir, bu da onu örneğin uçak motor bileşenleri gibi karmaşık kritik parçaların üretimi için çok uygun hale getirir. SLM, Üç Boyutlu (3D) Bilgisayar Destekli Tasarım (CAD) modeline göre metal tozlarını katman katman seçici olarak eritmek ve kaynaştırmak için odaklanmış bir lazer ışını kullanır. Bununla birlikte, SLM kullanılarak üretilen parçalar genellikle mekanik özelliklerinden taviz verebilecek belirli mikroyapısal kusurlar sergiler. Bunlar arasında artık gerilmeler, gözeneklilik ve tane sınırları ve çökeltiler gibi mikroyapısal kusurlar yer alır. Bu kusurların üstesinden gelmek ve SLM ile üretilen (SLMed) IN718'in mekanik özelliklerini iyileştirmek için ısıl işlem sonrası işlemler kullanılır. Bu çalışma, SLMed IN718 parçalarının mekanik davranışını (çekme ve sertlik), imalat yönünü ve homojenizasyon tavlaması ve yeni yaşlandırma dahil olmak üzere uygulanan ısıl işlemleri dikkate alarak incelemektedir. Bulgular, imalat sürecinin iyileştirilmesi ve yüksek sıcaklık bileşenlerinde istenen mekanik özelliklerin elde edilmesi için değerli bilgiler sunmaktadır. AM tekniklerinin uygun ısıl işlemlerle birleştirilmesi, yüksek performans gereksinimleri için karmaşık geometrilere sahip net şekilli IN718 parçaları üretmek için büyük bir potansiyele sahiptir.

Anahtar Kelimeler: Inconel 718, Süper Alaşım, Katmanlı İmalat, Havacılık ve Uzay, Seçici Lazer Eritme.

EXTENDED ABSTRACT

IN718 is a nickel-based superalloy commonly used in high-temperature applications due to its exceptional mechanical properties and resistance to environmental degradation. It exhibits high strength, excellent fatigue and creep resistance, oxidation resistance, and favorable weldability at elevated temperatures. These properties make it a preferred material for critical components in industries such as aerospace, automotive, nuclear, and petrochemical.

Traditionally, IN718 has been produced and applied through forging, casting, and powder metallurgy. However, with the increasing demand for high precision, integration, and complex configurations of IN718 components, traditional casting and forging methods may not meet the demanding process requirements. Therefore, the application of new machining methods is necessary for the precise production of IN718 parts with complex geometries and high-performance requirements. Additive Manufacturing (AM), also known as Three-Dimensional (3D) printing, is a new machining method that is attracting great interest in Aerospace and automotive industry. It enables the production of complex geometries with high material customizations and shorter production time compared to traditional manufacturing techniques.

It is one of the various AM techniques available. Selective Laser Melting (SLM) is a promising technique for producing high-temperature components, including IN718, using metal powders fused layer by layer based on a 3D CAD model. SLM offers several advantages, such as high geometric complexity, material utilization, and reduced production time.

However, laser-induced heat-affected zones in parts produced with SLM may contain mechanical and microstructural defects, such as residual stresses, porosity, grain boundaries, and precipitates. To overcome these limitations and improve the mechanical properties of SLM-produced (SLMed) IN718, post-production heat treatments are widely used.

IN718 parts produced with AM require an additional heat treatment called precipitation hardening to achieve the desired strength. This process is crucial for achieving high tensile strength and consists of three stages: homogenization, solution, and aging. During homogenization, the material is held at approximately 1100°C for 1-2 hours before being cooled in air or a faster environment to remove residual stresses and induce grain growth. The next stage is the solution treatment, which dissolves all phases into the austenite phase. This process is completed by cooling the material in air or faster for at least 1 hour between 954 and 982°C, resulting in increased ductility and toughness. For the aging process, the material is first kept in an oven at approximately 720°C for 8 hours. Then, the material is allowed to cool in the furnace to 620°C in a controlled manner at a cooling rate of 5°C/hour. To complete the aging process, the material must be cooled in air or by a faster method at 620°C for 10 hours. This practice increases the strength and hardness of the material.

Ermaksan produced the samples for this study using the SLM method with 15-45 μm IN718 powder material. The laser speed was 800 mm/s, laser power was 220 W, laser spot diameter was 0.085 mm, and layer thickness was 0.03 mm. A total of 12 specimens were produced, with 6 specimens each in the vertical and horizontal production directions. The specimens underwent mechanical cleaning to remove support burrs. Two different heat treatments were applied in the laboratory of Çukurova University's Department of Mechanical Engineering to enhance the mechanical properties of the specimens.

Our study implemented a shorter heat treatment process to improve the mechanical properties of IN718 specimens produced with AM, resulting in cost and time savings. A single Homogenization annealing was formed by combining homogenization and solution processes, followed by a single-step heat treatment instead of a two-step aging heat treatment.

For the initial heat treatment, two specimens in each production direction were left untreated, while the remaining specimens (four horizontal and four vertical) underwent Homogenization annealing. The specimens were heated to 1170°C at a rate of 10°C/min and held at this temperature for 2 hours before being allowed to cool in air. In the second heat treatment, two homogenization samples from each production direction were subjected to aging heat treatment. The samples underwent heat treatment by heating them to 750°C at a rate of 10°C/min and maintaining this temperature for 10 hours, followed by cooling with water.

This resulted in 12 samples of 6 different types produced using SLM and subjected to 2 different heat treatments. The specimens were labelled as follows: AsBuilt Vertical (V-AsB), AsBuilt Horizontal (H-AsB), Homogenized Vertical (V-HA), Homogenized Horizontal (H-HA), New-Aging Vertical (V-NA), or New-Aging Horizontal (H-NA).

To enhance the manufacturing process and achieve the desired mechanical properties for high-temperature applications, we conducted a study on microstructure and mechanical behavior of SLMed IN718. We considered the effects of manufacturing direction and post-heat treatment processes. We performed tensile, hardness, and X-ray Fluorescence Spectrometer (XRF) tests on each sample. XRF testing was conducted on all specimens to determine material proportions.

The specimens were subjected to tensile testing using a Zwick-Roell Z250 testing machine. The stress-strain plots obtained were compared with eah other and Raw IN718 (Rw IN718) and ErmakA241-INC718 (ER-IN718) data.

In the horizontal direction, the yield stress of the NA specimen increased by approximately 44% compared to the AsBuilt specimens. Similarly, the tensile stress increased by 28%. Also, there was a 26% decrease in elongation. In the vertical production direction, the NA specimen exhibited a 46% increase in yield stress compared to the AsBuilt specimens, as well as a 27% increase in tensile stress, but a 22% decrease in elongation. As for the Rw IN718 specimen, there was a 2% increase in yield stress, a 12% decrease in tensile stress, and a 4% decrease in elongation compared

to the H-NA specimen. The yield stress of the V-NA specimen decreased by approximately 13%, while the tensile stress decreased by 25% and the elongation increased by 14%.

In comparison to the ER-IN718 Horizontal production data, the yield stress of the H-NA specimen increased by approximately 48%, while the tensile stress increased by 15%, but the elongation decreased by 4%. When compared to the ER-IN718 vertical production data and V-NA specimen, the yield stress increased by approximately 50%, while the tensile stress increased by 7% and the elongation decreased by 5%.

Hardness measurements were taken on the surfaces of each specimen and compared with the hardness values of Rw IN718 and ER-IN718. Five measurements were taken for each surface of the specimen, and the average of these values was evaluated. The NA samples were found to be harder than both Rw IN718 and ER-IN718 in both production directions.

Among the AsBuilt specimens, H-AsB exhibited the highest hardness, suggesting an advantage in the horizontal built direction in the AsBuilt state. HA specimens showed that V-HA had the lowest hardness, while H-HA had the highest. This indicates that the vertical built direction negatively affected the material properties after HA treatment. Additionally, all NA specimens had higher hardness than their as-built or HA counterparts, with H-NA having the highest average hardness of all groups. The AsBuilt state exhibited a medium level of hardness in both horizontal and vertical specimens, measuring 375 HV and 333 HV, respectively. HA treatment resulted in a decrease in hardness for both horizontally and vertically built specimens, with V-HA exhibiting the lowest hardness of all groups at 292 HV. The hardness of both horizontal and vertical directions increased with the NA treatment, with H-NA exhibiting the highest hardness among all groups (386 HV). The heat treatment significantly affected the hardness properties of Inconel 718, with the order of hardness from highest to lowest being NA, AsBuilt, and HA. Additionally, the horizontal specimens had slightly higher hardness than the vertical specimens.

The experiments demonstrated that the aging heat treatment significantly enhanced the tensile strength of horizontally produced specimens, whereas annealing improved the elongation of vertically produced specimens. After comparing the results of tensile, hardness, and XRF tests with similar studies, it can be concluded that AM produces parts with higher mechanical properties than conventional methods. However, this is dependent on the heat treatments applied, the intended use, and the direction of production. The H-NA showed a 6% increase in hardness and a 28% increase in tensile strength compared to samples produced by AM without heat treatment. In contrast, the vertically annealed specimen showed a 9% decrease in hardness but a 37% increase in elongation. The results indicate that heat treatment can improve the mechanical properties of IN718 parts with high temperature resistance, making them suitable for aerospace and defense applications.

The study concludes that additive manufacturing technologies, such as SLM, have significant potential to produce IN718 components with complex geometry and high performance demands when combined with appropriate post-heat treatment processes.

GENİŞLETİLMİŞ ÖZET

IN718, olağanüstü mekanik özellikleri ve çevresel bozulmaya karşı direnci nedeniyle çeşitli yüksek sıcaklık uygulamalarında yaygın olarak kullanılan nikel bazlı bir süper alaşımdır. IN718 yüksek sıcaklıklarda yüksek mukavemet, mükemmel yorulma ve sürünme direnci, oksidasyon direnci ve uygun kaynaklanabilirlik sergiler. Bu özellikler onu havacılık, otomotiv, nükleer ve petrokimya gibi endüstrilerdeki kritik bileşenler için tercih edilen bir malzeme haline getirir.

Geleneksel olarak IN718 dövme, döküm ve toz metalurjisi formlarında üretilmiş ve uygulanmıştır. Bununla birlikte, IN718 bileşenlerinin yüksek hassasiyet, entegrasyon ve karmaşık konfigürasyonlarına yönelik artan taleple birlikte, geleneksel döküm ve dövme yöntemleri zorlu süreç gereksinimlerini karşılayamayabilir. Bu nedenle, karmaşık geometrilere ve yüksek performans gereksinimlerine sahip IN718 parçalarının net şekilde üretimi için yeni işleme yöntemlerinin uygulanması gereklidir. Havacılık ve otomotiv endüstrisinde büyük ilgi gören bu tür yeni işleme yöntemlerinden biri Katmanlı Üretimdir (AM). Üç Boyutlu (3D) baskı olarak da bilinen AM, geleneksel üretim tekniklerine kıyasla yüksek malzeme özelleştirmeleri ve daha kısa üretim süresi ile karmaşık geometrilerin üretimine olanak tanır.

Çeşitli AM teknikleri arasında Seçici Lazer Eritme (SLM), IN718 de dahil olmak üzere Ni bazlı yüksek sıcaklık bileşenlerinin üretimi için uygun potansiyele sahiptir. SLM, metal tozlarını 3D CAD modeline göre katman katman seçici olarak eritmek ve kaynaştırmak için odaklanmış bir lazer ışını kullanır. Bu teknik, yüksek geometrik karmaşıklık, yüksek malzeme kullanımı ve azaltılmış üretim süresi gibi benzersiz avantajlar sunar.

Bununla birlikte, SLM ile üretilen parçalarda lazer etkisiyle oluşan ısıl etkili bölgelerde mekanik ve mikroyapısal kusurlar ortaya çıkar. Bunlar arasında artık gerilmeler, gözeneklilik ve tane sınırları ve çökeltiler gibi mikroyapısal kusurlar yer alabilir. Bu kusurların üstesinden gelmek ve SLM ile üretilen IN718'in mekanik özelliklerini iyileştirmek için, üretim sonrası ısıl işlemler yaygın olarak kullanılmaktadır.

Geleneksel olarak AM ile üretilen IN718 parçalarda, istenen mukavemeti elde etmek için çökeltme sertleştirmesi olarak bilinen ek bir ısıl işlem gerektirir. Bu işlem, yüksek gerilme mukavemetine ulaşmak için çok önemlidir. Bu işlem üç aşamadan oluşur: homojenizasyon, çözelti ve yaşlandırma. Homojenizasyon sırasında malzeme havada veya daha hızlı bir ortamda soğutulmadan önce 1-2 saat boyunca yaklaşık 1100°C'de tutulur ve artık gerilmeleri gidermek ve tane büyümesini sağlamak için uygulanır. Çözelti işlemi, östenit fazındaki tüm fazları çözen bir sonraki aşamadır. Bu işlem, malzemenin 954 ila 982°C arasında en az 1 saat boyunca havada veya daha hızlı bir şekilde soğutulmasıyla tamamlanır ve süneklik ve tokluğun artmasını sağlar. Yaşlandırma işlemi için malzeme ilk olarak 8 saat boyunca 720°C civarında bir fırında tutulur. Daha sonra, malzeme fırında 5°C/saat soğutma hızıyla kontrollü bir şekilde 620°C'ye kadar

soğumaya bırakılır. Yaşlandırma işleminin tamamlanması için malzemenin havada veya daha hızlı bir yöntemle 10 saat boyunca 620°C'de soğutulması gerekir ve malzemenin mukavemetini ve sertliğini artıran bir uygulamadır.

Bu çalışma için numuneler Ermaksan tarafından SLM yöntemi ile 15-45 μm IN718 toz malzemeden, lazer hızı 800 mm/s, lazer gücü 220 W, lazer spot çapı 0,085 mm ve katman kalınlığı 0,03 mm parametreleri kullanılarak üretilmiştir. Dikey ve yatay üretim yönlerinde 6'şar adet olmak üzere toplam 12 adet numune üretilmiştir. Üretilen numuneler, destek çapaklarını gidermek için mekanik temizliğe tabi tutulmuştur. Numunelerin mekanik özelliklerini iyileştirmek için iki farklı ısıl işlem uygulanmış ve ısıl işlemler Çukurova Üniversitesi Makine Mühendisliği Bölümü laboratuvarında gerçekleştirilmiştir.

Yaptığımız çalışmada, AM ile üretilen IN718 numunelerin mekanik özelliklerini iyileştirmek için maliyetten ve zamandan tasarruf ederek daha kısa bir ısıl işlem uygulaması hazırladık. Homojenizasyon ve çözelti işlemleri birleştirilerek tek bir homojenleştirme tavlaması oluşturulmuş ve ardından iki aşamalı yaşlandırma ısıl işlemi yerine tek basamaktan oluşan bir ısıl işlem uygulanmıştır.

İlk ısıl işlem için, her bir üretim yönündeki iki numune olduğu gibi bırakılırken, kalan numuneler (dört yatay ve dört dikey) gerilim giderme tavlamasına tabi tutulmuştur. Numuneler 10°C/dk ısıtma hızıyla 1170°C'ye ısıtılmış ve 2 saat boyunca bu sıcaklıkta tutulduktan sonra havada soğumaya bırakılmıştır. İkinci ısıl işlemde, her üretim yönünden 2 adet gerilim giderme ısıl işlemine tabi tutulan numune, yaşlandırma ısıl işlemine tabi tutulmuştur. Numuneler 10°C/dk ısıtma hızıyla 750°C'ye ısıtılmış, 10 saat bu sıcaklıkta tutulduktan sonra suyla soğutulmuştur.

Isıl işlemler sonucunda SLM kullanılarak üretilen ve 2 farklı ısıl işleme tabi tutulan 6 farklı tipte 12 numune elde edilmiştir. Numuneler aşağıdaki gibi kodlanmıştır: AsBuilt Dikey (V-AsB), AsBuilt Yatay (H-AsB), Homogenized Dikey (V-HA), Homogenized Yatay (H-HA), New-Aging Dikey (V-NA), or New-Aging Yatay (H-NA).

Üretim sürecini optimize etmek ve yüksek sıcaklık uygulamaları için istenen mekanik özellikleri elde etmek amacıyla, SLMed IN718'in mikroyapısı ve mekanik davranışı, üretim yönünün ve ısıl işlem sonrası işlemlerin etkileri dikkate alınarak incelenmiştir. Her bir numune üzerinde çekme, sertlik ve X-ışını floresan spektrometresi (XRF) testleri yapılmıştır. XRF testi tüm numuneler üzerinde gerçekleştirilmiş ve malzeme oranları belirlenmiştir.

Numuneler Zwick-Roell Z250 test cihazında çekme testine tabi tutulmuştur. Elde edilen gerilme-gerinim grafikleri döküm IN718 (Rw IN718) ve ErmakA241-INC718 (ER-IN718) verileri ile karşılaştırılmıştır.

Yatay imalat yönünde, NA numunesinin akma gerilmesi AsBuilt numunelerine kıyasla yaklaşık %44 oranında artmıştır. Benzer şekilde, çekme gerilmesi de %28 oranında artmıştır. Ayrıca, uzamada %26'lık bir azalma olmuştur. Dikey üretim yönünde, NA numunesi, AsBuilt numunelerine kıyasla akma gerilmesinde %46'lık bir artış, çekme gerilmesinde %27'lik bir artış,

ancak uzamada %22'lik bir azalma sergilemiştir. Rw IN718 numunesinde ise H-NA numunesine kıyasla akma gerilmesinde %2'lik bir artış, çekme gerilmesinde %12'lik bir düşüş ve uzamada %4'lük bir azalma görülmüştür. V-NA numunesinin akma gerilmesi yaklaşık %13 oranında azalırken, çekme gerilmesi %25 oranında azalmış ve uzama %14 oranında artmıştır.

ER-IN718 Yatay üretim verileriyle karşılaştırıldığında, H-NA numunesinin akma gerilmesi yaklaşık %48 artarken, çekme gerilmesi %15 artmış, ancak uzama %4 azalmıştır. ER-IN718 dikey üretim verileri ve V-NA numunesi ile karşılaştırıldığında, akma gerilmesi yaklaşık %50 artarken, çekme gerilmesi %7 artmış ve uzama %5 azalmıştır.

Her bir numunenin yüzeyinde sertlik ölçümleri alınmış ve Rw IN718 ve ER-IN718 sertlik değerleri ile karşılaştırılmıştır. Numunenin her bir yüzeyi için beş ölçüm alınmış ve bu değerlerin ortalaması değerlendirilmiştir. Yaşlandırılmış numunelerin her iki üretim yönünde de hem Rw IN718 hem de ER-IN718'den daha sert olduğu bulunmuştur.

AsBuilt numuneler arasında H-AsB en yüksek sertliği sergilemiştir, bu da AsBuilt durumunda yatay imalat için bir avantaja işaret etmektedir. HA numuneler V-HA'nın en düşük sertliğe, H-HA'nın ise en yüksek sertliğe sahip olduğunu göstermiştir. Bu da dikey inşa yönünün HA işleminden sonra malzeme özelliklerini olumsuz etkilediğini göstermektedir. Buna ek olarak, tüm NA numuneler AsBuilt veya HA daha yüksek sertliğe sahipti ve H-NA tüm gruplar arasında en yüksek ortalama sertliğe sahipti. AsBuilt durumu, hem yatay hem de dikey numunelerde orta düzeyde sertlik sergilemiş ve sırasıyla 375 HV ve 333 HV ölçülmüştür. HA işlemi her iki üretim yönünde sertlikte bir düşüşe neden olmuş ve V-HA 292 HV ile tüm gruplar arasında en düşük sertliği sergilemiştir. NA işlemi ile her iki yönde de sertlik artmış ve H-NA 386 HV ile tüm gruplar arasında en yüksek sertliği sergilemiştir. Isıl işlem Inconel 718'in sertlik özelliklerini önemli ölçüde etkilemiş, sertlik sıralaması en yüksekten en düşüğe doğru NA, AsBuilt ve HA olmuştur. Ayrıca, yatay numuneler dikey numunelerden biraz daha yüksek sertliğe sahipti.

Deneyler, NA ısıl işleminin yatay olarak üretilen numunelerin çekme mukavemetini önemli ölçüde artırdığını, tavlamanın ise dikey olarak üretilen numunelerin uzamasını iyileştirdiğini göstermiştir. Çekme, sertlik ve XRF testlerinin sonuçları benzer çalışmalarla karşılaştırıldığında, AM, uygulanan ısıl işlemlere, kullanım amacına ve üretim yönüne bağlı olarak geleneksel yöntemlerden daha yüksek mekanik özelliklere sahip parçalar ürettiği sonucuna varılabilir. Isıl işlem uygulanmadan AM ile üretilen numunelerle karşılaştırıldığında, H-NA sertlikte %6 ve çekme mukavemetinde %28 artış göstermiştir. Buna karşılık, V-NA sertlikte %9'luk bir düşüş, ancak uzamada %37'lik bir artış sergilemiştir. Bulgularımız, havacılık, uzay ve savunma sanayi uygulamalarında kullanılacak yüksek sıcaklık dayanımına sahip IN718 parçalar için uygulanan ısıl işlemler sonucunda daha iyi mekanik özellikler elde edilebileceğini göstermiştir.

Bu çalışma, SLM gibi eklemeli üretim teknolojilerinin, uygun ısıl işlem sonrası süreçlerle birleştirildiğinde, karmaşık geometriye ve yüksek performans taleplerine sahip IN718 bileşenleri üretmek için önemli bir potansiyele sahip olduğu sonucuna varmaktadır.

ACKNOWLEDGEMENTS

I would like to extend my endless thanks to my family, who have always been behind me throughout my education life, who have given me all their support on this path and have an important share in getting me to this point.

I would also like to thank Ermaksan for the production of the spesimens used in this study and Cem DOĞAN and Seyit Halil TURGUT for helping me with the mechanical tests.

LIST OF TABLES

Table 1.1 The composition of some of the most common superalloys (Reed, 2008) 3
Table 1.2 Mechanical properties of superalloys (Nickel Institute, 2021; MatWeb, 2023; ASM, 2023) 4
Table 1.3 Physical & mechanical properties of IN718 (ASM, 2023) 5
Table 1.4 The composition of IN718 (ASM, 2023) 5
Table 3.1 Powder characterization (Ermaksan, 2023) 21
Table 3.2 Powder composition (weight percent) 22
Table 3.3 SLM manufacturing parameters 23
Table 4.1 Measured powder characterization 31
Table 4.2 The chemical composition of the specimens with weight percentages 32
Table 4.3 Hardness measurements for surface #A on x-axis 39
Table 4.4 Hardness measurements for surface #A on Y-axis 40
Table 4.5 Hardness measurements for surface #B on x-axis 40
Table 4.6 Hardness measurements for surface #B on y-axis 41
Table 4.7 Hardness measurements for surface #C on x-axis 41
Table 4.8 Hardness measurements for surface #C on y-axis 42
Table 4.9 Hardness measurements for surface #D on x-axis 43
Table 4.10 Hardness measurements for surface #A on Y-axis 43
Table 4.11 Tensile test results 46
Table 4.12 Hardness test results 47

LIST OF FIGURES

Figure 1.1 Material used in a gas turbine engine (Dawood and Salim, 2021) 2
Figure 1.2 Inconel flanges (Priminox, 2023) 2
Figure 1.3 Inconel alloy pipe fittings (Yizeng Pipe, 2023) 2
Figure 1.4 Example of crystal structure of superalloys, γ" (Ni3Nb) (Surface Centred Tetragonal) (Wikipedia, 2023) 6
Figure 1.5 Classification of the alloying elements in Ni-based superalloy. (Long, 2018) 6
Figure 1.6 Components made of inconel used in aircraft engines, (a) spool, (b) shaft, (c) combustion casing, (d) turbine disc (Coromant, 2023) 7
Figure 1.7 AM process steps (Gibson et al. 2015) 9
Figure 1.8 Classification of AM processes from different contexts (Alghamdi, 2021). 10
Figure 1.9 Schematic representation of some AM methods (Yan et al. 2020) 10
Figure 1.10 Selective laser melting, (Razavykia et al. 2020) 11
Figure 1.11 (a) Gas turbine exhaust mixing nozzle made by laser enhanced net forming (LENS), (b) Compressor support element for a gas turbine engine made by electron beam melting (EBM), (c) Turbine blade with internal cooling channels made by SLM, (d) Turbine blades made by SLM, (e) Hollow static turbine blade casting using molds and cores made by SLM, (f) Engine casing made by SLM. (Guo, 2013) 12
Figure 1.12 IN718 temperature-time-transformation diagram (Radavich, J. F., 1989) 14
Figure 3.1 Enavision series 3D metal printer used in this study 21
Figure 3.2 Particul and powder of IN718 22
Figure 3.3 Dimensions of the test specimen 23
Figure 3.4 Image of lazer beam for horizontal specimens 24
Figure 3.5 Production of horizontal specimens 24
Figure 3.6 Vertical and horizontal building direction of samples 24
Figure 3.7 Vertical (a) and horizontal (b) Specimens 25
Figure 3.8 Homogenization annealing (HA) 26
Figure 3.9 New aging heat treatment (NA) 27
Figure 3.10 Specimens subjected to the heat treatment 27
Figure 3.11 Zwick-Roell Z250 tensile test machine 28
Figure 3.12 Specimens subjected to tensile test 28
Figure 3.13 Surface codes and direction of hardness measuring lines 29
Figure 3.14 The indentation images 29
Figure 4.1 Results of XRF analysis 32
Figure 4.2 Stress-Strain curve of asbuilt state 33

Figure 4.3 Stress-Strain curve of homogenized specimen 34
Figure 4.4 Stress-Strain curve of new-aged specimen 34
Figure 4.5 Stress-Strain curves of horizontally built specimens 35
Figure 4.6 Fractured specimens after tensile test 35
Figure 4.7 Stress-Strain curve of asbuilt state 36
Figure 4.8 Stress-Strain curve of homogenized specimen 36
Figure 4.9 Stress-Strain curve of new-aging specimen 37
Figure 4.10 Stress-Strain curve of vertical specimens 38
Figure 4.11 Fractured specimens after tensile test 38
Figure 4.12 Average vickers hardnesses 44

SYMBOLS AND ABBREVIATIONS

IN718 : Inconel 718
AM : Additive Manufacturing
3D : Three Dimensional
CAD : Computer Aided Design
SLM : Selective Laser Melting
ER-IN718 : ErmakA241-INC718
SLMed : SLM-produced
LENS : Laser Enhanced Net Forming
EBM : Electron Beam Melting
ASTM : American Society for Testing and Materials
HIP : Hot Isostatic Pressing
XRF : X-ray fluorescence spectrometer
AMS : Aerospace Material Standards
MPa : Megapascal
μm : Micrometre
γ : Gamma
δ : Delta
EBSD : Electron Backscatter Diffraction
NHT : Novel Heat Treatment
NA : New Aged
DA : Double Aging
HA : Homogenization Plus Aging
SA : Solution Plus Aging
S : Stress Reliefed
STL : Stereolithography
PMI : Positive Material Identification
AsB : AsBuilt
V : Vertical
H : Horizontal
HV : Vickers Hardness

1. INTRODUCTION

1.1. Overview of Superalloys and Applications

Superalloys are materials known for their exceptional performance at high temperatures, making them ideal for high temperature applications. These alloys retain their mechanical properties even when subject to elevated conditions in excess of 650°C for prolonged periods of time. Superalloys are specifically designed for high-temperature environments and possess remarkable corrosion and oxidation resistance, as well as superior friction and durability at elevated temperatures (Bhattacharya, 1983).

The versatility of superalloys arises from their exceptional combination of elevated-temperature strength, cryogenic ductility, and superior surface stability. The term 'superalloy' was invented just after World War II to identify a group of materials engineered for turbochargers and aero turbomachinery where high temperature performance was important (Sims et al., 1987). The use of superalloys in extreme conditions is advantageous due to their ability to improve the efficiency and reduce the fuel consumption of modern turbine systems (Reed, 2006).

Applications for superalloys can be listed as follows:

- Aerospace and industrial gas turbine parts include disks, pins, shafts, propellers, vanes, combustors, afterburners, and engines. Figure 1.1 shows material used in a gas turbine engine,
- Steam turbine power plant parts: bolts, propellers, flue gas auxiliary heaters,
- Automotive parts: turbo-compressors, exhaust valves,
- Metal working materials: high temperature resistant working tools and molds, casting molds,
- In medical equipment: dental, prosthetic devices,
- Spacecraft parts: aerodynamic heated surfaces, rocket motor parts,
- Heat treatment parts: fixtures, conveyor belts,
- Control rod drive mechanisms, valves, and piping systems are found in nuclear power plants,
- Bolts, fittings, reactors, piping and pumping are all used in the chemical and petrochemical industry, Figure 1.2 and Figure 1.3 shows the examples of flanges and fitting made by Inconel alloys.

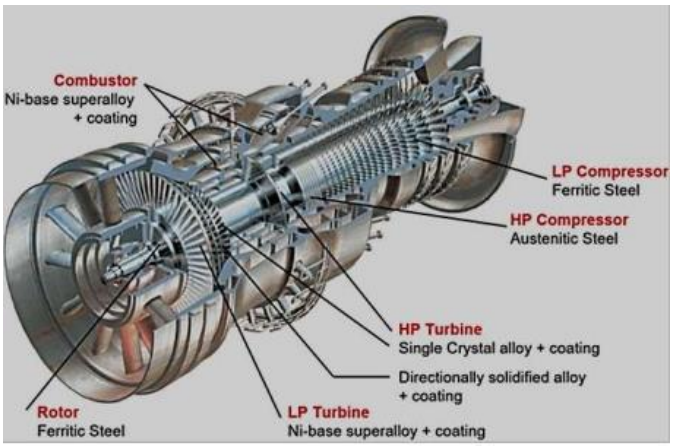


Figure 1.1 Material used in a gas turbine engine (Dawood and Salim, 2021)



Figure 1.2 Inconel flanges (Priminox, 2023)



Figure 1.3 Inconel alloy pipe fittings (Yizeng Pipe, 2023)

There are three basic classes of high-temperature superalloys: nickel-base, iron-nickel-base, and cobalt-base (Donachie, 2000). Iron-nickel base superalloys have lower strength than nickel base alloys. Due to their high melting point, these materials are stronger than iron and nickel. Nickel-base and cobalt-base superalloys are preferred in applications where service life is long and mechanical stress is high. Depending on the strength required, iron-nickel superalloys are more commonly used than cobalt- or nickel-base superalloys due to their lower cost at lower

temperatures (Donachie, 2000). The material composition of some of the most common superalloys can be seen in Table 1.1.

Table 1.1 The composition of some of the most common superalloys (Reed, 2008)

Alloy	**Fe**	**Ni**	**Co**	**Cr**	**Nb**	**Ta**	**Mo**	**W**	**Al**	**Ti**
Nickel-based Alloys										
IN-718	19,0	53,0	--	19,0	5,2	--	3,0	--	6,6	0.8
Mar-M 247	--	62,0	10,0	8,2	--	3,0	0.6	10,0	5,5	1,4
Udimet-700	--	53,0	19,0	15,0	--	--	5,2	--	4,3	3,5
CM SX-2	--	66,0	4,6	8,0	--	5,8	0.6	7,8	5,6	0.9
IN 713C	--	74,0	--	12,0	2,0	--	4,2	--	6,1	0.8
PWA 1480	--	63,0	5,0	10,0	--	12,0	--	4,0	5,0	1,5
Waspaloy	--	58,0	13,0	19,0	--	--	4,3	--	1,3	3,0
N-4	--	63,0	7,5	9,2	0.5	4,0	1,0	6,0	3,8	4,5
Rene 150	--	58,0	12,0	5,0	--	6,0	1,0	5,0	5,5	--
Cobalt-based Alloys										
HS-188	3,0	22,0	39,0	22,0	--	--	--	14,0	--	--
X-40	--	10,0	54,0	25,0	--	--	--	7,5	--	--
Iron-based Alloys										
A-286	53,0	26,0	--	15,0	--	--	1,3	--	0.2	2,2
N-155	30,0	20,0	20,0	21,0	1,0	--	3,0	2,5	--	--
CG-27	38,0	38,0	--	13,0	0.6	--	5,5	--	1,5	2,5

Nickel-based superalloys are known for their high strength, thermal and corrosion resistance, machinability, shape memory, and low coefficient of thermal expansion. Cobalt-based superalloys, on the other hand, have a higher melting point than nickel or iron-based alloys, superior hot corrosion resistance compared to nickel or iron-based alloys, and higher thermal fatigue resistance and weldability compared to nickel-based alloys. Iron-based superalloys exhibit high strength at room temperature and are highly resistant to creep, oxidation, corrosion, and abrasion. Tablo.1.2 shows the mechanical properties of superalloys (Nickel Institute, 2021; MatWeb, 2023; ASM, 2023)

High temperature strength combined with corrosion resistance is setting the standard for superalloy materials for biomedical devices (Donachie, 2000). In particular, cobalt-based superalloys are widely used in medical and dental implants. Haynes 25 is a cobalt-based superalloy known to be used in gas turbine hot sections, nuclear reactor parts and medical applications. Haynes 188 and S-816 cobalt-based alloys are used in high pressure turbine blades and gas turbine combustors (Davis, 2000).

Nickel-base superalloys such as IN718, which gain strength through precipitation hardening, are utilized in highly demanding applications like gas turbine engines. Iron-nickel superalloys like A-286 and Incoloy 901 series are also used in gas turbine engines, specifically in turbine blades, discs, and shaft parts.

Table 1.2 Mechanical properties of superalloys (Nickel Institute, 2021; MatWeb, 2023; ASM, 2023)

Nickel-based alloys	**Ultimate Tensile Strength, MPa**	**Yield Strength, MPa**	**Elongation at Break,** %
IN-718	1375	1100	25
Mar-M 247	1119	980	4.8
Udimet-700	703	400	18
CM SX-2	1055	890	16
IN 713C	968	734	7.16
PWA 1480	905	1140	12
Waspaloy	1335	910	26.6
N-4	462	148	47
Rene 150	450	-	45
Cobalt-based alloys			
HS-188	946	464	53
X-40	548	453	34
Iron-based alloys			
A-286	620	275	40
N-155	550	310	18
CG-27	231	154	56

1.2. Mechanical Behavior of Inconel 718

Inconel 718 can show superior mechanical properties, as shown on Table 1.3, and it is a nickel-iron alloy with a nominal composition of 50-55% Ni, 17-21% Cr, 4.75-5.5% Nb, 2.8-3.3% Mo, 0.65-1.15% Ti, 0.65-1.15% Co, 1% Co, with minor additions of Al and Fe, which can be seen in Table 1.4. The alloy is designed for strength, creep resistance and good fatigue life at elevated temperatures up to 700°C and is known to have good weldability due to its relatively slow precipitation kinetics. Because of its exceptional strength at elevated temperatures, excellent fatigue, wear and hot corrosion resistance and good weldability, it is used in a wide range of high temperature applications in aircraft, gas turbines, turbocharger rotors, nuclear reactors, liquid fuelled rockets and a variety of other corrosive and structural applications in the form of castings, forgings and powder metallurgy products.

Table 1.3 Physical & mechanical properties of IN718 (ASM, 2023)

Physical Properties	
Density	8.19 g/cc
Mechanical Properties	
Tensile Strength, Ultimate	1375 MPa
Tensile Strength, Ultimate at Elevated Temperature	1100 MPa
Tensile Strength, Yield	1100 MPa
Tensile Strength, Yield at Elevated Temperature	980 MPa
Elongation at Break	25 %
Elongation at Break at Elevated Temperature	18 %

Table 1.4 The composition of IN718 (ASM, 2023)

Component	Al	Co	Cr	Cu	Fe	Mn	Mo	Nb	Ni	P	S	Si	Ti
Wt. %	0.2 - 0.8	Max 1	17 - 21	Max 0.3	17	Max 0.35	2.8 - 3.3	4.75 - 5.5	50 - 55	Max 0.015	Max 0.015	Max 0.35	0.65 - 1.15

Superalloys, such as IN718, are excellent candidates for use in turbine disks, compressor blades, cryogenic storage tanks, high-pressure vessels, and piping due to their exceptional corrosion resistance, high-temperature strength, and weldability (Sims, 1984). These alloys have a surface-centered cubic austenite crystal structure and are grouped as Rene, Hastelloy, and Inconel alloys (Figure 1.4). The properties conferred by the elements in nickel-based single crystal superalloys can be classified under four groups: base group elements, mechanical strength group elements, long-term stability group elements, and oxidation resistance group elements (Figure 1.5) (Long, 2018). Inconel is a group of nickel-chromium based superalloys that exhibit excellent mechanical properties under extreme conditions. These properties are due to their high tensile strength, yield strength, corrosion resistance, and creep resistance. Thanks to the passive film layer formed by this alloy, it can withstand the effects of corrosion, high temperature, and pressure. Additionally, its mechanical properties can be improved through heat treatments such as solid solution and precipitation hardening (Mouritz, 2012).

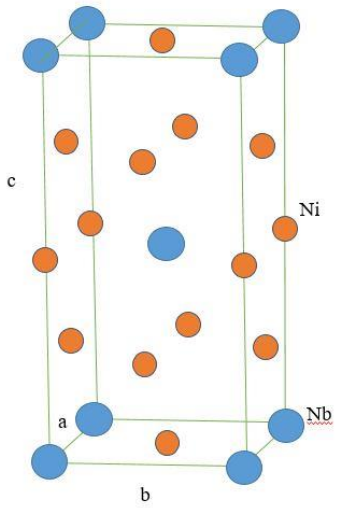


Figure 1.4 Example of crystal structure of superalloys, γ" (Ni3Nb) (Surface Centred Tetragonal) (Wikipedia, 2023)

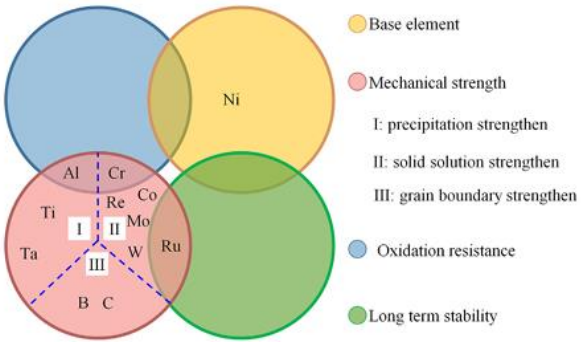


Figure 1.5 Classification of the alloying elements in Ni-based superalloy. (Long, 2018)

Nickel-based superalloys are commonly used in the aerospace, defense, and automotive industries for manufacturing key components such as turbine blades, seals, fasteners, engine shafts, pressure vessels, and nuclear reactor parts. These materials are crucial to many industries and are typically produced using traditional manufacturing methods.

1.3. Importance in Aerospace, Automotive, Nuclear, and Petrochemical Industries

Nickel-based alloys are extensively utilized in various industries such as aerospace, chemical, automotive, space, and medical due to their exceptional mechanical and physical properties (Korkmaz et al., 2005). Nickel-based superalloys constitute 50% of advanced technology aircraft engines. They are utilized in a variety of high-temperature applications, including aircraft propulsion systems, industrial gas turbines, spaceships, aerospace rocket motors, power reactors, submersibles, steam generating plants, and the petrochemical industry, mainly because they retain their strength for long periods at temperatures above 700°C (Warbuton, 1967). Alloys containing elements such as molybdenum, tungsten, niobium, aluminum, titanium, etc. have been developed

which significantly increase the resistance of nickel-based alloys. Udimet Alloy 720 (UD720), Inconel Alloy 600 (IN600), and Inconel Alloy 718 (IN718) are the most commonly used alloys.

It exhibits excellent mechanical properties, good corrosion resistance, and high-temperature ductility (Davis, 2000). IN718 is a widely used superalloy in the aerospace, reactor, and petroleum industries in both cast and wrought forms. The alloy's strength is enhanced by heat treatment through a precipitation hardening mechanism. (Slama C. and Abdellaoui M., 2000).

IN718 was first developed by the International Nickel Corporation during the 1950s. It is widely used for materials used in extreme condition applications, especially aircraft and gas turbines. IN718 possesses important properties such as high-temperature resistance, oxidation and corrosion resistance, and ease of forging and welding (Kuo et al., 2009). Some components made of Inconel material and used in aircraft engines can be seen in Figure 1.6.

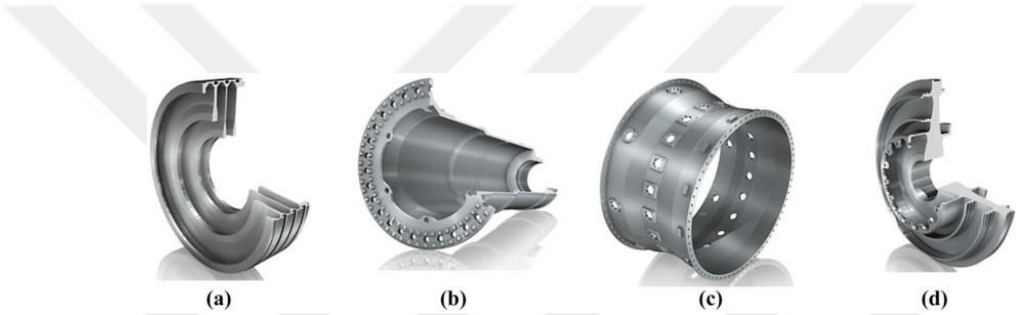


Figure 1.6 Components made of inconel used in aircraft engines, (a) spool, (b) shaft, (c) combustion casing, (d) turbine disc (Coromant, 2023)

1.4. Manufacturing Methods and Their Limitations for Complex Geometries

IN718 is the most important and widely used of these nickel-based superalloys. IN718 is a superalloy: It refers to high strength, heat resistant alloys in which some elements such as cobalt, chromium, etc. are added to the nickel-based alloy which contains 18% to 20% of iron.

The most widely used of the traditional manufacturing methods is machining. However, significant difficulties are encountered in the manufacturing process of nickel-based superalloy materials by machining (Zhou, J., et al. 2012). Due to the properties of these materials, such as maintaining their strength at extreme conditions, low thermal conductivity coefficients and their ability to harden, their production by traditional manufacturing methods is costly and difficult (Li, L., et al., 2015). These properties also cause problems such as tool wear during forming, high cutting forces and deterioration of dimensional accuracy. In addition, the production of complex shaped and in some cases thin-walled parts, such as aircraft parts used in aviation, is more difficult and the production costs are significantly higher (Arunachalam, 2004).

Therefore, the use of AM methods instead of traditional manufacturing methods (casting, machining, forging, etc.) is becoming increasingly important for components made from IN718 material. Like stainless steels, IN718 and other nickel-base superalloys have inferior machinability

characteristics. However, it is possible to machine IN718 in the solution or aged condition by selecting the appropriate cutting material, method, speed, and depth of cut. The annealed alloy solution offers improved machinability and longer insert life during machining, while the aged alloy promotes more chip formation and results in a better surface finish at the end of the machining process.

The machining of IN718 is challenging due to its high strength and work hardening. During machining, the presence of hard carbides in the microstructure can cause abrasive wear on the insert, leading to increased machining costs (Klopp, 1995).

1.5. The Need for Net Shape Production

IN718 is classified as a difficult-to-machine alloy due to the high cutting forces caused by hardening during machining and the high tool temperatures caused by its low thermal conductivity. The properties of aero engine alloys make them challenging to machine. When machining IN718, it is crucial to consider parameters such as insert type, processing method, machining speed and the penetration depth of the cutting edge.

Producing IN718 parts using conventional methods can be challenging, and achieving the desired shapes often comes at the cost of sacrificing good material properties, such as high-temperature corrosion and creep resistance. The material must be pre-annealed to achieve easy machining, forging, and welding, as well as ductility and improved formability.

In addition, the production of complex shaped and in some cases thin-walled parts such as aerospace aircraft parts are more difficult, and the production costs are significantly higher (Arunachalam, 2004). The use of AM methods is becoming increasingly important for components made from IN718 material, replacing conventional manufacturing methods such as casting, machining, and forging.

1.6. Introduction to Additive Manufacturing and SLM

AM, also referred to as rapid prototyping and 3D printing, is a manufacturing process that enables the production of parts with complex geometries by combining and layering materials, as opposed to the machining process of traditional manufacturing methods (Frazier et al. 2014). Because of these capabilities, it is moving toward replacing traditional manufacturing methods. In the future, it is expected to have widespread use, especially in Aerospace industry.

Compared to conventional manufacturing methods, AM, i.e. 3D printing, which is achieved by adding materials layer by layer, offers a number of advantages (Özsoy and Duman, 2017).

- The capability to manufacture intricate components with shapes that are not feasible to produce using traditional methods,

- The capacity to shorten the manufacturing development process and the capacity to produce small quantities of components in a limited period of time and with a limited amount of financing,
- Cost savings by optimizing material usage,
- Ability to produce functionally graded parts.

AM begins with the creation of a 3D CAD file on a computer, which is then converted into a standard AM file format, such as STL or other AM formats. The file is then transferred to an AM machine, where the position and orientation of the part are controlled, and the part is produced in layers. Finally, the part undergoes AM post-processing, if necessary. Figure 1.7 illustrates the steps involved in the AM process.

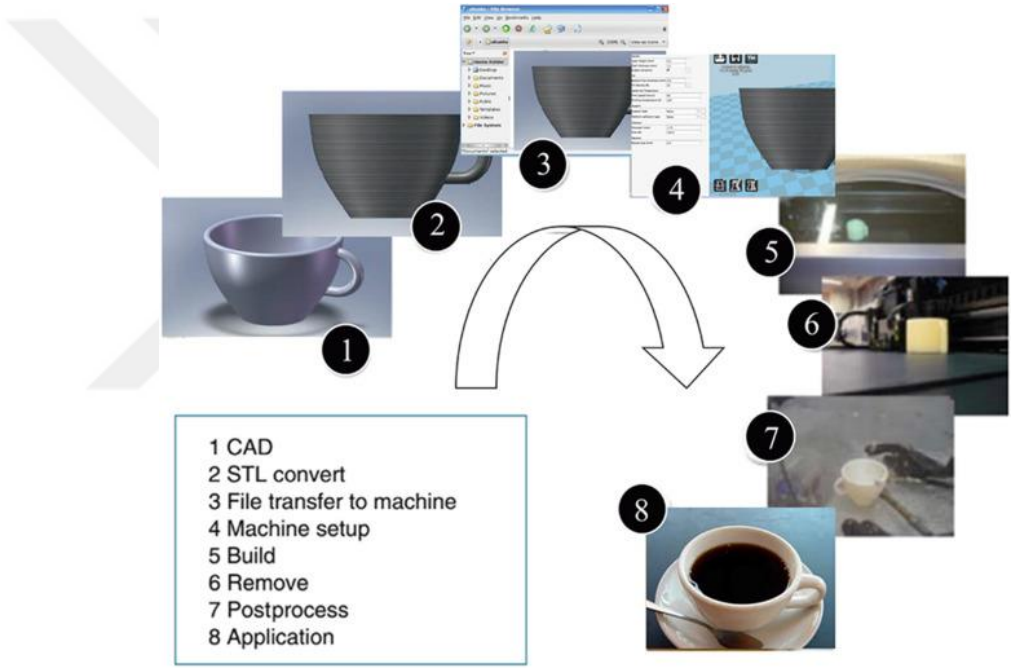


Figure 1.7 AM process steps (Gibson et al. 2015)

The production processes of AM can be classified into three groups, as shown in Figure 1.8. The technologies are defined based on the methodology of product formation, the type of base material used, and the processing medium.

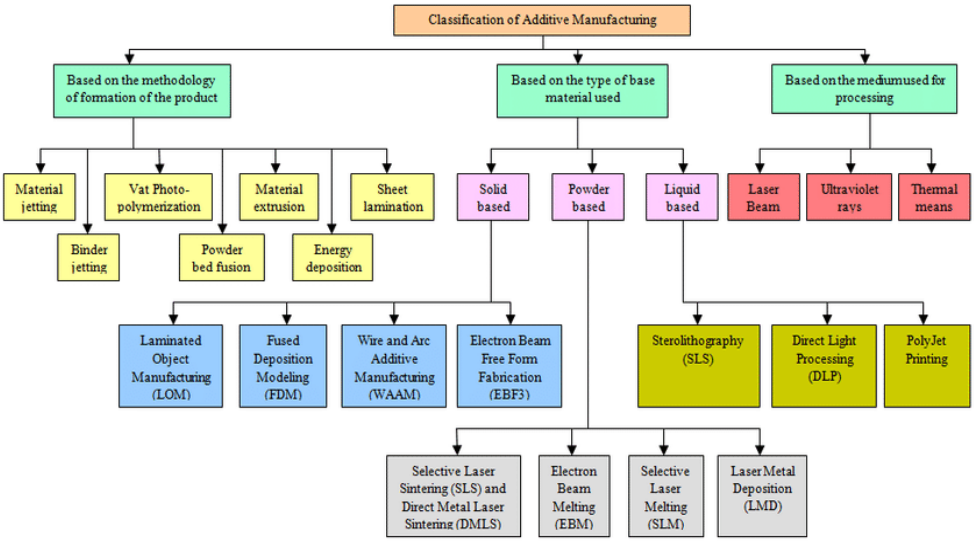


Figure 1.8 Classification of AM processes from different contexts (Alghamdi, 2021).

There are many different production methods according to the area of use and the results of the production. The schematic views of the most commonly used AM and production methods are as shown in Figure 1.9.

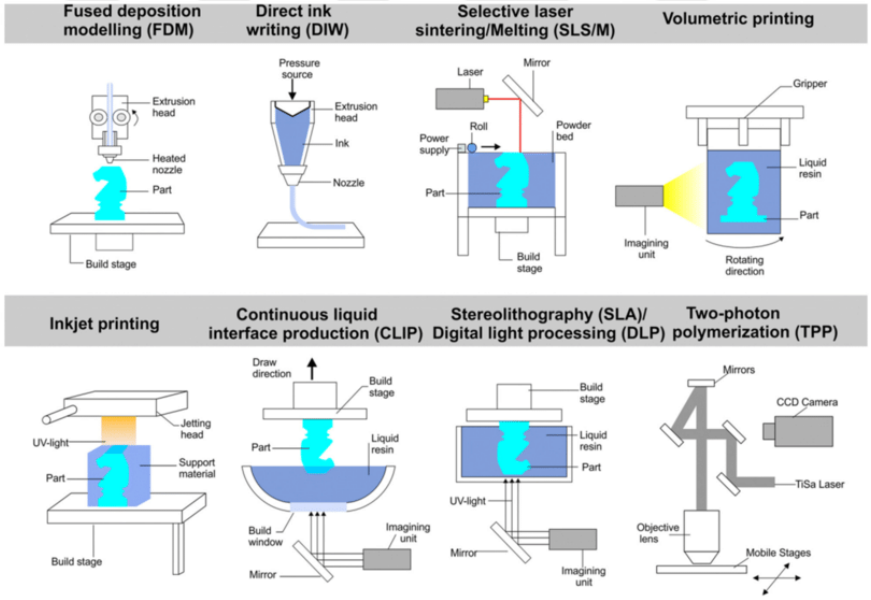


Figure 1.9 Schematic representation of some AM methods (Yan et al. 2020)

SLM is an additive manufacturing method used for 3D printing metal alloys. During the melting process, additional particles are created by mixing metal powder particles together. Similar to the SLS process, the metal part is produced layer by layer based on the 3D model. The SLM technique completely melts the powder and therefore requires a higher temperature compared to other metal 3D printing techniques. To create optimal melting conditions, the build chamber is filled with a noble gas such as argon or nitrogen. The complete melting process ensures the

formation of a uniform layer with high strength, making it ideal for pure metals like titanium or aluminum. Due to the high temperatures required for complete melting, cooling times are also lengthy.

As previously stated, AM is an advanced method of production that enables the creation of 3D parts layer by layer, directly from a CAD model, using powder or wire feedstock, without requiring any part-specific tools or knowledge (Yalçın and Ergene, 2017). A laser or electron beam is typically used to selectively melt or sinter the feedstock. It involves melting a section of the powder design with a laser and adding a new layer of powder on top, which is then melted and added to the previous layer. The schematic view of the SLM method can be seen in Figure 1.10.

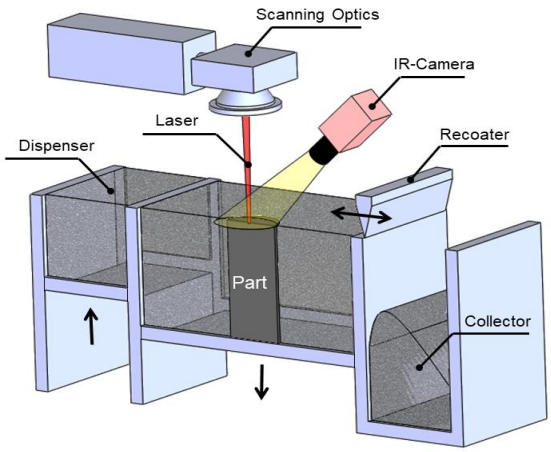


Figure 1.10 Selective laser melting, (Razavykia et al. 2020).

IN718 parts, which are widely used in Aerospace industry, are subjected to various dynamic loads at extreme conditions. As a result, the surface and subsurface properties that occur after production seriously affect the performance and fatigue life of the parts. Poor surface and subsurface properties formed in the parts after production limit the direct use of the components. To overcome this problem, it is necessary to select optimum parameters. However, despite the determination of optimum parameters, if the parts do not meet the desired properties in the area where the parts will be used, secondary processes are performed in addition to the parts (Sunay, 2020). While some of the surface improvement processes affect the surface of the material, some of them can also change the mechanical properties such as wear, corrosion, residual stress, fatigue by affecting the subsurface properties of the parts. Examples of the SLMed turbine parts can be seen in Figure 1.11.

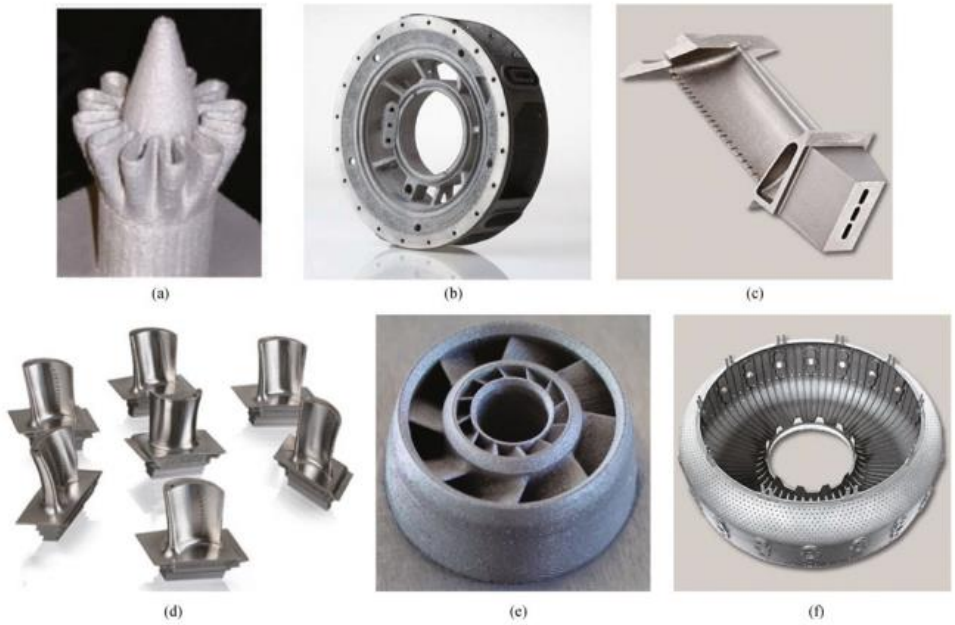


Figure 1.11 (a) Gas turbine exhaust mixing nozzle made by laser enhanced net forming (LENS), (b) Compressor support element for a gas turbine engine made by electron beam melting (EBM), (c) Turbine blade with internal cooling channels made by SLM, (d) Turbine blades made by SLM, (e) Hollow static turbine blade casting using molds and cores made by SLM, (f) Engine casing made by SLM. (Guo, 2013)

Parts made from IN718 are one of the most difficult alloys to form. IN718, which is widely used in Aerospace industry, is difficult to produce in series and it is difficult to produce multiple parts as a single component. AM is an important alternative to overcome these difficulties. For this reason, industries such as aerospace, defense and biomedical have attached great importance to AM methods. In other words, it can be difficult to achieve the desired designs with conventional manufacturing. This means that component performance can be compromised when using conventional manufacturing methods as it can affect mechanical performance properties such as high temperature corrosion and creep resistance. An annealing step is also required at the start of any machining, forging or welding process. AM of IN718 has shown that mechanical properties are not compromised and can even exceed those of cast or forged parts.

In contrast, metal AM makes IN718 easier to machine and ensures good retention of material properties. Despite the variety of AM methods recently developed, SLM is much more widely used than other methods. SLM is an advanced AM process for producing metal machines from metal powders. SLM is a powder bed fusion process that selectively melts and fuses powder sections layer by layer using a high-intensity laser, based on CAD data. However, parts produced by SLM may experience thermal stress, distortion, and high surface roughness.

1.7. The Effect of Post Heat Treating on the Mechanical Characteristics

Heat treatment involves heating and cooling metals to improve their mechanical properties, such as hardness and strength. Specific temperatures and durations are applied to the parts during

this metallurgical process, resulting in a specific phase and trapping granules in the microstructure of the part in a non-equilibrium phase at room temperature through cooling in different environments. Heat treatment has been a long-standing method to enhance the properties of parts produced through conventional manufacturing techniques (Kim, H., et al., 1997). By applying heat treatment to parts produced through AM, it is possible to reduce the porous structure caused by insufficient melting and residual stresses (Wang, X. and K. Chou, 2019).

Heat treatment can improve the mechanical properties of superalloy materials produced by AM. To achieve optimal mechanical performance, parts must undergo a specific period of time under appropriate temperature conditions, followed by appropriate cooling conditions. These processes alter the concentration ratios of elements in the superalloy and significantly impact the microstructure of the IN718 alloy, including grain size. In the temperature-time-transformation diagram below, Figure 1.12, the changes in the chemical structure of the material depending on temperature and time can be seen. Heat treatment information for IN718 produced by SLM generally follows the guidelines of ASTM F3055-14a, which are based on processes developed for wrought and cast materials. This standard recommends homogenization at 1065ºC for 1.5 hours. Optional hot isostatic pressing (HIP) can be done in the temperature range of 1120ºC to 1185ºC for 4 hours and at a pressure of at least 100 MPa. This should be followed by solution annealing and double aging, as specified in AMS 2774 (ASTM F3055−14a, 2014; AMS 2774A, 2005), which involves heating at 815-1010ºC for 1 hour and aging at 718ºC for 8 hours, followed by aging at 621ºC for 10 hours.

The heat treatment process for SLM-generated materials is more complex than that for forged or cast materials, typically requiring longer heating times and higher temperatures. Research by Huang et al. (1996) showed that applying heat treatment at 1066ºC reduced the formation of Laves and δ phases in IN718 parts. Tucho (2017) conducted a study on the impact of heat treatment on IN718 parts. The study discovered that extending the heating time at both 1100ºC and 1250ºC caused growth of grains and carbides in the matrix.

In the temperature range of 730 to 1040 ºC, secondary carbides precipitate and can affect the alloy's mechanical properties. Undesirable δ phases with needle-like morphologies may also form (Raghavan, S., et al., 2017). Therefore, it is crucial to accurately optimize the size, shape, and volume ratios of γ' and γ'' phases, as well as the ageing temperature and time, to determine the microstructure and mechanical performance. It has been discovered that after heat treatment of IN718 parts produced using SLM, a significant amount of carbide forms alongside the γ' and γ'' phases, as well as the needle-shaped δ phase. The heat-treated parts exhibit superior mechanical properties when compared to non-heat-treated parts (Raghavan, S., et al., 2017). A study investigated the influence of different ageing temperatures on the mechanical properties of IN718 parts produced by SLM. According to Huang et al. (2019), the most favourable mechanical

properties were achieved through ageing at temperatures between 680 and 720 ºC. This was due to the formation of strengthening phases (γ' and γ").

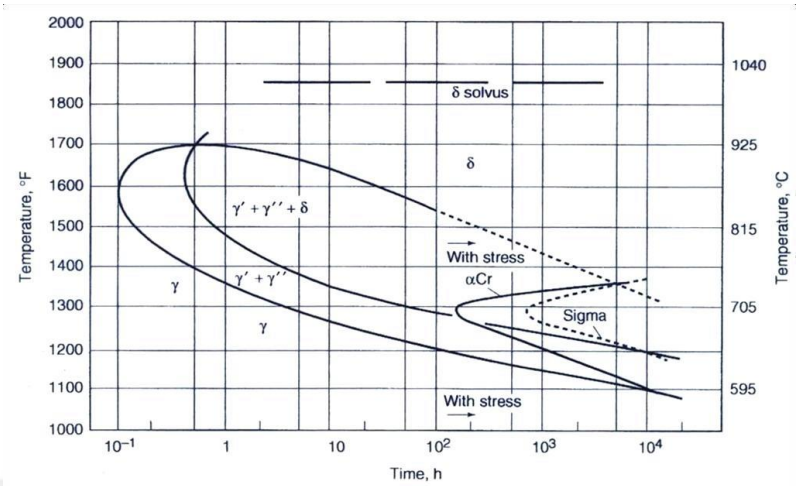


Figure 1.12 IN718 temperature-time-transformation diagram (Radavich, J. F., 1989)

This study investigates the fabrication of IN718 material suitable for high temperature applications using SLM, a type of AM capable of producing complex geometries, and analyzes the mechanical behavior of SLMed IN718 considering the effects of fabrication direction and post-production heat treatment processes on the material. The objective is to provide valuable information for optimizing the manufacturing process of IN718 to achieve the desired mechanical properties at elevated temperatures in a shorter time and at a lower cost.

2. LITERATURE REVIEW

Numerous studies have been conducted on the design and manufacturing of IN718 superalloy using AM. This section specifically examines studies of additively manufactured IN718 and the impact of heat treatments on AM-produced IN718 materials, particularly SLM.

Poyraz and Kuşhan (2018) suggest that the use of AM for metallic materials is gaining popularity in design and manufacturing. In addition to design and manufacturing, AM also offers benefits in maintenance and repair. One of the most significant advantages is the ability to obtain metallurgical and mechanical properties comparable to the original part material in worn areas.

Another study evaluated residual stresses, distortions, plastic stresses, and maximum temperature values using the Amphyon 2021 AM simulation program. The study used the SLM process to investigate the fabrication of scaffolds and implant core structures for the biomedical field with different fill ratios. The results indicate that plastic stresses can predict crack formation and tend to concentrate in the corner regions. In addition, cellular structures have higher maximum temperatures compared to solid structures. The study found that parts with higher relative densities have higher maximum temperatures up to a certain structure height. However, once this height is reached, parts with lower density experience higher maximum temperatures. This leads to the localization of plastic stresses between the first layer of the part and the supporting structure. The findings have significant implications for the optimization of design and stress analysis in the manufacturing of cellular structures for biomedical applications using SLM (Ergene, 2022).

Hosseini and Popovich (2019) discovered that the mechanical properties of AM IN718 is influenced by various parameters, such as the AM method, fabrication process parameters, heat treatment parameters, structure configuration, and direction of manufacturing. Furthermore, the fatigue performance of AM IN718 was inferior to that of wrought alloy due to AM melting defects and poor surface quality. Research indicates that optimizing parameters for the AM process, along with subsequent heat and surface treatments, can significantly enhance the fatigue strength of AM IN718. This can exceed that of wrought materials.

Amato et al. (2012) studied IN718 cylinders produced by SLM using argon or nitrogen gas and pre-alloyed powder. The cylinder structures were analyzed using optical metallography, TEM, and X-ray diffraction techniques. The cylinders exhibited a specific architecture of phase deposits. After annealing, 50% of the material recrystallised and precipitates and some d-phase deposits were observed in the recrystallisation zones. The hardness values of the cylinders were determined to assess their mechanical properties. The values obtained were 33RC in their original manufactured state, 39RC after HIP treatment, and 40RC for the annealed material. These values are comparable to the hardness values of the wrought IN718 alloy.

Trosch et al. (2016) investigated the production of semi-finished IN718 parts using various manufacturing techniques. Tensile test specimens were prepared and tested at different

temperatures (room temperature, 450°C, and 650°C). The results showed that the SLM process produces parts with better mechanical properties than forgings and castings at room temperature. The material treated with SLM showed similar properties to forgings at high temperatures. Additionally, a significant amount of intragranular δ-phase was observed in the SLM-treated material.

Peng et al. (2023) conducted a study on the microstructure and mechanical properties of an IN718 superalloy produced using SLM technology. They investigated the wear behavior of the alloy at different temperatures. The study found that the grains in the alloy produced by SLM are more uniformly distributed along the horizontal axis. Additionally, the material exhibited slightly higher microhardness in the horizontal plane compared to the vertical plane. The tensile test results show that the alloy has higher tensile strength in the horizontal direction, but slightly lower elongation. The primary factor that affects the fracture mechanism of the material is the aggregation of micropores. The friction wear tests indicate that the friction wear coefficient of the alloy decreases as the temperature increases. At elevated temperatures, abrasive wear, oxidative wear, and adhesive wear are the main wear mechanisms detected. Therefore, it has been concluded that the IN718 alloy improves its resistance to friction and wear by forming a protective oxide layer at high temperatures.

The literature shows that the key parameters for producing components from IN718 powders using the SLM method are laser scanning speed, laser power, scanning strategies, layer thickness, and laser focus diameter (Liverani et al., 2017). These parameters impact various properties of the parts. A study on the production process of IN718 parts with SLM showed that different scanning strategies resulted in changes in porosity ratios, mechanical properties, and residual stress values of the parts. Laser power and laser scanning speed parameters, in particular, resulted in significant differences in material properties. Research in the literature has shown that the laser scanning speed plays a crucial role in the formation of porosity defects in IN718 parts (Choi et al., 2017). Additionally, laser energy density, which is affected by both laser scanning speed and laser power, has a significant impact on surface topography and quality (Jia, Q. and D. Gu, 2014).

Konečná and Nicoletto (2019) conducted a study on the fatigue performance of SLM IN718. They applied stresses in various directions based on the structure's orientation, using specimens produced by two different SLM systems. The fatigue test results were interpreted with the aid of metallography and fractography studies. The study concluded that the manufacturing parameters of the SLM system and the printing strategy significantly affect the fatigue response of IN718. The fatigue performance of SLM IN718 is anisotropic in its AsBuilt condition, mean that it depends on the direction of the applied stresses relative to the build orientation. The fatigue fracture mechanism is determined by the combination of stress, surface roughness, and near-surface microstructure.

Huang et al. (2019) conducted a study on the microstructure and mechanical properties of IN718 material produced by the SLM process. The study analysed the effects of solution temperature, time, cooling rate, and age hardening on IN718. The results indicated that IN718 produced by SLM has a unique microstructure compared to cast and forged materials, and therefore requires different processing. The study demonstrates that decreasing the cooling rate during solution treatment aids in the precipitation of reinforcement phases. Additionally, it indicates that the microstructure of SLMed IN718 can be adjusted to modify its tensile properties. The maximum elongation rate is attained after solution treatment without aging, whereas the highest yield and tensile strength are achieved after aging. By adjusting the cooling rate and aging time of the solution treatment, the amount of reinforcing phases can be controlled to achieve compatibility between strength and ductility.

In 2001, Greene and Finfrock conducted a study on the oxidation properties of IN718. The study involved exposing samples to oxidation at different temperature ranges. After the oxidation period, the samples were weighed to measure the increase in mass due to oxygen uptake. The study identified three different oxidation regimes for IN718. Passivation was observed in the low-temperature regime after the initial transient oxidation period of the samples. The study found that in the medium-temperature regime, oxidation was limited by diffusion. However, in the high-temperature regime, rapid oxidation caused material deformation and damage. This research enhances our understanding of the high-temperature oxidation behaviour of IN718.

Li et al. (2019) proposed a new heat treatment scheme for the IN718 superalloy processed by SLM. The study investigated the microstructural and mechanical properties of AsBuilt, hot isostatic pressing (HIP), and NHT specimens. The NHT specimen achieved an improved strength-ductility synergy that could not be achieved by conventional HIP treatment. The elongation was greatly improved from 17% to 24% with little loss in ultimate strength (1325 MPa vs. 1320 MPa). Annealing twins enhance plasticity in recrystallized grains, while finer γ' and γ" precipitates aid in maintaining high levels of strength.

Zhang et al. (2015) investigated the effects of standard heat treatments on the microstructure and mechanical properties of SLM-treated IN718 alloy. The tests were based on AM standards for cast and wrought IN718 alloy. The raw specimens formed dislocated cellular structures due to interdendritic Laves precipitates and the absence of γ´ and γ" phases, resulting in transgranular fracture. Although the strength of the raw specimens was lower than that of the treated specimens, their ductility was better. The mechanical strength of the material increased after undergoing solution annealing treatment. However, its ductility decreased significantly due to the reduction caused by precipitate phases in the austenitic matrix. Conversely, after undergoing HAS treatment, there was little change in strength and hardness, but a small decrease in yield strength occurred. The ductility of the material increased due to the decrease in δ precipitate phases.

Deng et al. (2018) investigated the microstructural and mechanical properties of SLM IN718 alloy during fabrication and heat treatment. The study found that the alloy has a fine celldendritic microstructure during fabrication, with fine Laves phase precipitations observed in the intradendritic regions. The matrix contains a high density of dislocations but no γ′/γ″ phases. During electron backscatter diffraction (EBSD) analyses, it was observed that cellular dendrites grew epitaxially at the melt pool boundaries and then competed inside. This resulted in irregular grains elongated along the build direction and a poor texture. The vertically fabricated IN718 samples exhibited lower strength than the horizontally fabricated samples but showed greater ductility. After heat treatment, the samples showed an increase in strength and a decrease in ductility. This study provides insight into the influence of manufacturing and heat treatment conditions on the microstructure and mechanical properties of SLM IN718 alloy.

Candioto et al. (2015) conducted a study to characterise superalloy IN718 after a double aging heat treatment. The superalloy underwent a solution treatment at 1095°C for 1 hour, followed by a double aging treatment at 955°C for 1 hour, and finally at 720°C for 8 hours and 620°C for 8 hours. The alloys were characterized using scanning electron microscopy/backscattered electron mode (SEM/BSE) and traditional X-ray diffraction (XRD) with an Oxford Instruments energy dispersive X-ray spectrometry system. The double ageing process resulted in a larger grain size compared to that of the IN718.

Xu et al. (2023) highlighted the significance of post-heat treatment in the production of nickel-based superalloys for aerospace applications using laser powder deposition. Their study revealed that the use of constant laser power deposition and gradient laser power deposition methods results in different microstructures. The study showed that when laser power is deposited on samples with finely discrete Laves phases and low segregation rates, it results in a homogeneous distribution of elements and the formation of specific phases through standard dissolution. On the other hand, when laser power is deposited on samples with coarse long-chain Laves phases and high segregation rates, high temperature treatments are required to ensure homogeneous element distribution. Heat treatments were found to significantly affect the fracture mechanism of the samples. Both specimens underwent a transition from a ductile transgranular fracture mode to a mixed mode of transgranular and intergranular fractures after direct ageing and heat treatment.

Kuo et al. (2009) studied phase precipitation in a sample aged at 955 ◦C for varying durations. The quantity of phase is directly proportional to the aging time. With longer aging times, the phase grains become more uniformly distributed and exhibit a more distinct orientation. If no phase forms, the tensile fracture life and creep elongation are longer compared to other process schemes. Grain boundary slippage is activated during creep testing. Phase-free specimens can exhibit high levels of creep elongation and typically display a ductile fracture pattern, indicating intergranular fracture.

Ageing is a significant process that accelerates the formation of the γ' and γ" phases, resulting in increased material strength. This strength improvement is attributed to the prevention of dislocation slip in the phases that form after the ageing process. In the heat-treated IN718 alloy, the volume fractions of γ' and γ" phases can vary, with γ' accounting for approximately 5% and γ" accounting for approximately 20% (Chamanfar et al., 2013). Strengthening phases (γ' and γ") have been observed to form at high temperatures, ranging from 700 to 900 ºC in some studies, and at lower temperatures, ranging from 550 to 660 ºC in others. The γ' phase typically forms at 620ºC, while the γ" phase generally forms at 720ºC (Thomas et al., 2006).

Jiang et al. (2024) conducted a study on the impact of solution annealing temperature and time on the mechanical properties of IN718 alloy. The results showed that solution annealing enhanced the tensile strength, yield strength, and density of the parts. However, higher solution treatment temperatures led to increased brittleness of the material, while longer solution treatment times improved the material's toughness. Additionally, the material's density increased with higher solution treatment time and temperature.

Jia and Gu (2014) analysed the densification behaviour, microstructural properties, microhardness, wear performance, and high-temperature oxidation properties of IN718 parts produced by the SLM method. The study investigated the relationships among processing conditions, microstructures, and material properties. The results showed that low laser energy density caused balling phenomena and decreased the density of the parts. Increasing the laser energy density resulted in achieving almost full density. The microstructures of IN718 parts machined using SLM underwent morphological changes as the laser energy density increased. Optimally machined parts exhibited a uniform distribution of microhardness, a low coefficient of friction, and a reduced wear rate. The worn surfaces showed the formation of an adhesive tribolayer, which improved wear performance. The study shows that the high-temperature oxidation resistance increased with the applied laser energy density. This improvement in oxidation resistance was attributed to the refinement of the microstructure architecture in the SLM-machined parts.

Li et al. (2018) investigated the microstructure development of IN718 alloy fabricated by SLM and exposed to various heat treatments. The microstructure and mechanical properties of the samples showed differences based on the manufacturing direction. Columnar and cellular substructures were observed in the overlap region, while only cellular substructure was observed in the center melting region in the section perpendicular to the building direction. Columnar structures were observed in the section parallel to the grain direction. Following the application of heat treatments, various phases were observed to form. The δ-Ni3Nb phases precipitated as a result of the decomposition of Nb and Ti during direct double aging (DA) treatment. Microsegregation and Laves phases, on the other hand, decreased with homogenization and double aging (HA) and

solution and double aging (SA) treatments. The analysis indicated that the SA sample exhibited the highest hardness value.

The manufacturing of metallic parts using the SLM method presents challenges such as residual stresses, distortion, and high surface roughness caused by melting and solidification. The literature offers various solutions to these issues. IN718 parts are commonly utilized in Aerospace industry and are subjected to dynamic loads at high temperatures. The performance of parts is significantly impacted by the surface and subsurface characteristics that form after production. Anisotropic properties that arise can restrict the direct use of components. To address this issue, it is necessary to select optimum parameters. However, even with optimal parameters, secondary operations may be required to achieve the desired properties for the intended use of the parts. Post-processing operations can impact the surface of the material and alter its mechanical properties. The literature review indicates that IN718 parts produced with AM exhibit structural and thermal stresses due to their manufacturing characteristics. To achieve better mechanical properties, various heat treatments are employed.

3. MATERIALS AND METHODS

3.1. Material

The IN718 specimens used in this study were manufactured by Ermaksan in Bursa. Ermaksan is the first Turkish company to produce metal 3D AM technology and offers innovative, high-quality, and high value-added products and solutions in the fields of sheet metal processing, AM, and optoelectronics. To achieve optimal quality in metal AM procedures and 3D printed products, it is crucial to characterize the feedstock powder. Particle size distribution plays an important role in final product quality and fatigue behaviour, dealing with surface finishing and density. To produce samples using SLM, we followed the powder supply and production parameters provided by the manufacturer. The IN718 powder particle size distribution characterized by ASTM B214 is shown in Table 3.1.

Table 3.1 Powder characterization (Ermaksan, 2023)

DESCRIPTION	
Particle size distribution per ASTM B214	
Particle Size (μm)	% By mass
>45	Max. 5.0
≤45	Max. 95.0

Twelve specimens, each measuring 120x10x6 mm, were manufactured using the EnaVision 3D Metal AM Machine through SLM, as depicted in Figure 3.1. The IN718 gas atomized powders, with an average particle size ranging from 15 to 45 μm, were used to manufacture the test samples in accordance with ASTM F3055, as shown in Table 3.2 (Ermaksan, Turkiye).



Figure 3.1 Enavision series 3D metal printer used in this study

For the samples to be produced with SLM, suitable powder supply and production conditions were provided by the manufacturer company. Production parameters and sample design

and dimensioning were done by us. The character and composition data of the IN718 powder used are as follows.

F3055. The manufacturer's the gas atomized powder ER-IN718 was used as the source powder with a chemical composition according to ASTM grain size indicates that the size of the particles is between 15 and 45 μm. Its Powder and pictures can be seen on Figure 3.2.

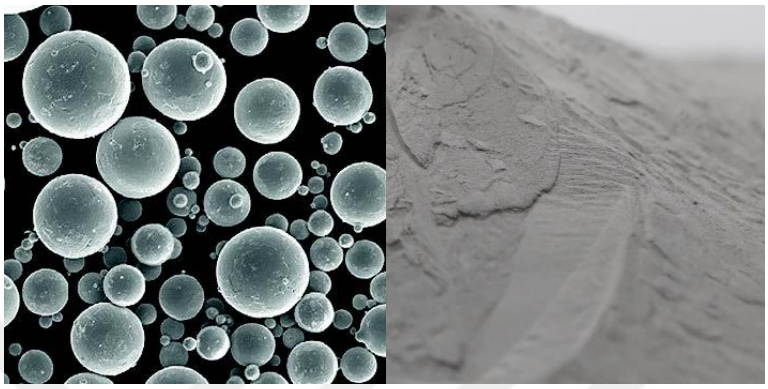


Figure 3.2 Particul and powder of IN718

Table 3.2 Powder composition (weight percent)

Element	**ASTM F3055**
Carbon (max)	0.08
Manganese (max)	0.35
Silicon (max)	0.35
Phosphorus (max)	0.015
Sulfur (max)	0.015
Chromium, range	17.0 - 21.0
Cobalt (max)	1.0
Molybdenum, range	2.80 - 3.30
Niobium + Tantalum	4.75 – 5.50
Titanium, range	0.65 – 1.15
Aluminum, range	0.20 – 0.80
Iron	Balance
Copper (max)	0.3
Nickel	50.00 – 55.00
Boron	0.006
Oxygen (max)	0.20
Nitrogen (max)	0.05

3.2. Production of the Samples

To examine the impact of process-related parameters on the mechanical performance of SLMed parts, we designed test specimens using Catia (Dassault Systèmes) software in accordance with the ASTM E8-E8M-2016 standard. This design was chosen due to the relatively small length of the specimens, which facilitates the manufacturing process. Figure 3.3 illustrates the basic dimensions of the designed specimens.

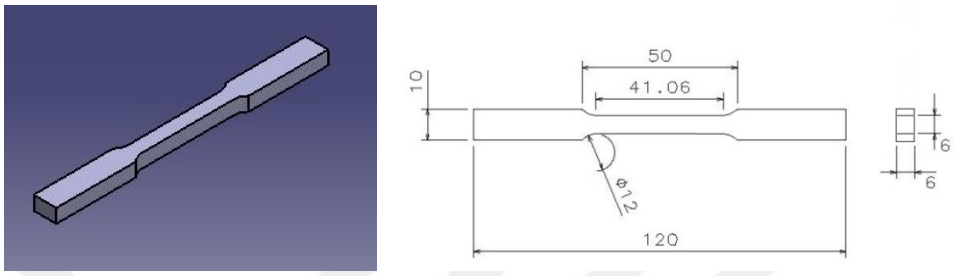


Figure 3.3 Dimensions of the test specimen

The samples are created using CAD software and then converted into Stereolithography (STL) format. Support structures are added to the STL component before being transferred to the EnaVision machine for production. The IN718 superalloy specimens were produced using the production parameters specified in Table 3.3. The machine used has a maximum power of 220W and a spot diameter of 85 μm. Sample dimensions of 120 mm x 10 mm x 6 mm are also shown in Figure 3.3.

Table 3.3 SLM manufacturing parameters

Production Parameters	**Values**
Laser Speed	800 mm/s
Laser Power	220 W
Laser Spot Diameter	0.085 mm
Layer Thickness	0.03 mm

The build plate was heated to 170°C for all specimens, and the process chamber was filled with argon gas (Ar) to ensure an oxygen concentration in the machine process camera lower than 10 ppmw, thus avoiding oxidation phenomena. The production process is illustrated in Figures 3.5 and 3.6.

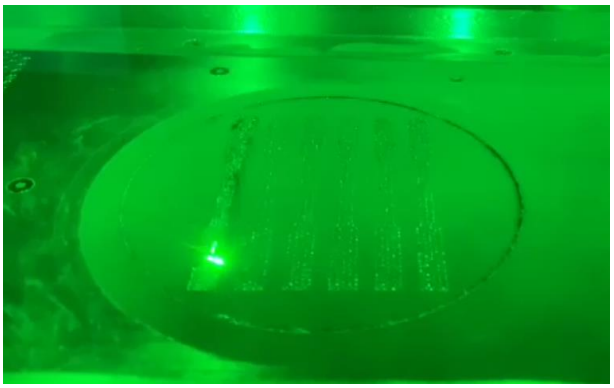


Figure 3.4 Image of lazer beam for horizontal specimens

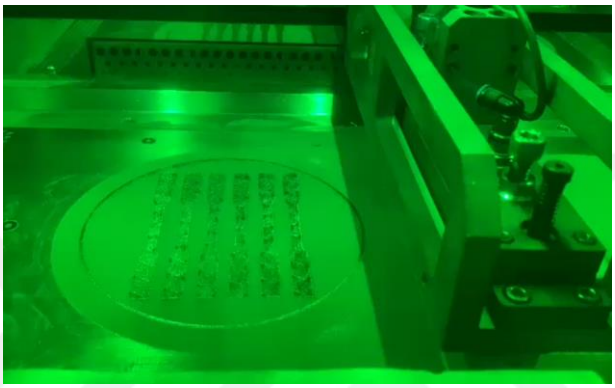


Figure 3.5 Production of horizontal specimens

The process requires depositing a thin layer of IN718 powder using a cylinder and melting it with a laser beam to bond it to the solidified regions below. The production plate is then moved down to repeat the process for a new layer of powder deposition and laser fusion. The laser strategy alternates scanning along the X and Y axes, with each layer having a different scanning direction.

3.3. Effects of Manufacturing Direction

Most SLM alloys exhibit anisotropy in various mechanical properties, depending on the building direction. To study the effects of anisotropy, we constructed test specimens with two axial orientations: 0° (vertical to the building direction) and 90° (parallel to the building direction). The building directions according to the axes are shown in Figure 3.6.



Figure 3.6 Vertical and horizontal building direction of samples

Twelve IN718 test specimens were produced using SLM, with six specimens in each direction. During production, support elements were created for the materials using software, and these support structures were removed after production. Post-production pictures of the vertical and horizontal specimens are shown in Figure 3.7. The specimens did not exhibit any significant distortion after being removed from the build chamber.



Figure 3.7 Vertical (a) and horizontal (b) Specimens

3.4. Heat Treatment Procedures

A significant characteristic of AM resides in microstructural anisotropy, resulting in a corresponding anisotropy in mechanical properties. The solidification structure, as formed during the AM building process, closely resembles that of a welded component, featuring readily apparent melting pools. The employment of a highly focused laser beam induces substantial thermal gradients, leading to the rapid solidification of thin layers and the subsequent development of columnar growth directed towards the thermal center of the laser spot. Consequently, a strongly segregated interdendritic zone is formed, accompanied by undesirable thermal stresses necessitating healing. In order to relieve residual stresses and modify the microstructure and mechanical properties as desired, the implementation of heat treatments becomes vital in the AM process.

The standard heat treatments for IN718 are Homogenization Annealing (HA), Solution Annealing (SA), and Double Artificial Ageing (AA). Wrought IN718 is typically treated with SA (980°C, 1 h/air cooling) and AA (720°C, 8 h/furnace cooling at 55°C/ 620°C, 8 h/air cooling)), while casting IN718 is treated with HA (1080°C, 1.5 h/air cooling) followed by SA and AA (Deng et al., 2018). Previous studies have shown that applying heat treatment to a temperature range of 1050-1150°C can recover interdendritic Nb microsegregation, which may otherwise lead to the formation of undesirable phases (Zhou et al., 2019). On the other hand, SA carried out at a lower temperature range of 925-1010°C cannot redissolve non-equilibrium phases that may precipitate during rapid solidification, hindering the homogenisation of the chemical composition (Li et al., 2018).

Further studies are required to optimize the homogenization and solution treatment conditions for SLMed IN718 due to the lack of published research on its heat treatment. Although most researchers have primarily employed conventional heat treatment methods for IN718 alloy manufactured through SLM, which have their limits. Conventional heat treatments are unable to address certain issues that persist in the post-treatment structure, such as residual stresses, micro-segregation of chemical composition, microstructural anisotropy, porosity, and surface roughness caused by laser utilization (Wang et al., 2019; Gao et al., 2018). The appropriate heat treatment should be chosen based on the parameters of the SLM process, the geometry and application areas of the produced parts, the magnitude of residual stresses, and the microstructure after the building process and post-production processing steps. To modify the microstructure, mechanical properties and reduce residual stresses, the SLMed IN718 samples subjected to a New Aging (NA) heat treatment, in addition to the use of HA.

For the first heat treatment, two specimens in each production direction were left untreated, while the remaining specimens (four horizontal and four vertical) were subjected to HA. The samples were heated to 1170°C at a rate of 10°C/min and held at this temperature for 2 hours before being allowed to cool to room temperature in air, as shown in Figure 3.9.

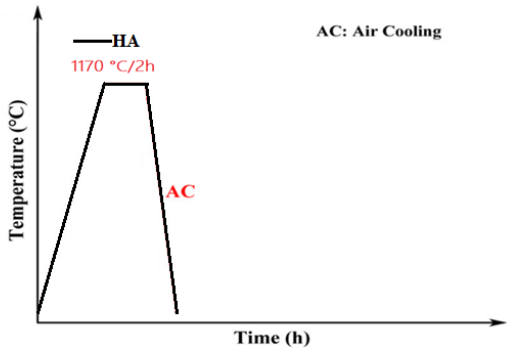


Figure 3.8 Homogenization annealing (HA)

For the second treatment, two specimens from each direction of production were selected from those that had undergone HA. These were then subjected to a new ageing heat treatment, known as NA. They were heated to 750°C at a rate of 10°C per minute and held at this temperature for 10 hours, then cooled to room temperature with water, as shown in Figure 3.9. The specimens before heat treatment are shown in Figure 3.10.

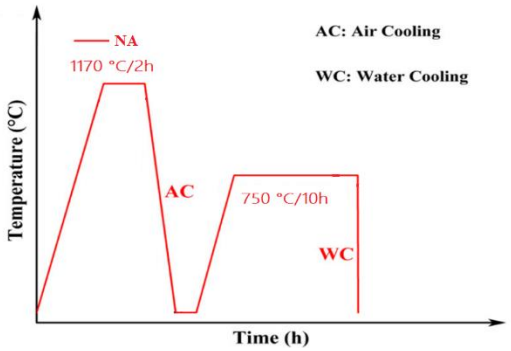


Figure 3.9 New aging heat treatment (NA)


Figure 3.10 Specimens subjected to the heat treatment

The specimens are numbered within each group. The first code indicates the first letter of the production direction, and the second code indicates the type of heat treatment used, such as AsBuilt Vertical (V-AsB), AsBuilt Horizontal (H-AsB), Homogenized Vertical (V-HA), Homogenized Horizontal (H-HA), New-Aging Vertical (V-NA), and New-Aging Horizontal (H-NA). After production by SLM and heat treatment processes, there are 12 samples in 6 different types.

3.5. Mechanical Tests

XRF Analysis, tensile and hardness tests were carried out to investigate the effect of build direction and post heat treatment on the mechanical performance of the SLMed IN718 part.

3.5.1. XRF Analysis

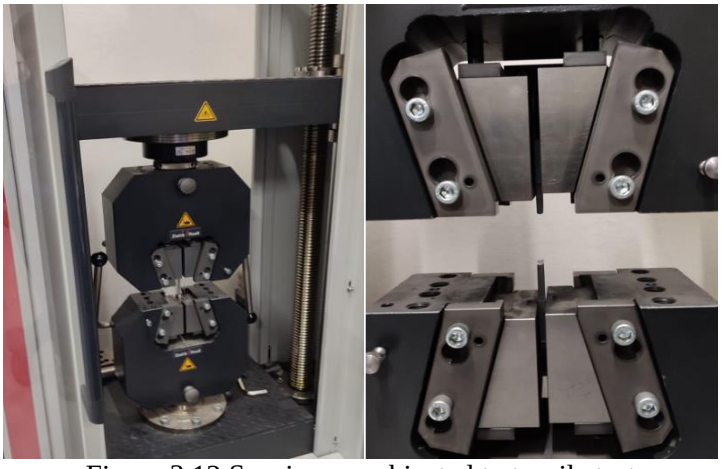
In order to observe the changes that may occur in the chemical composition of the material after manufacturing, the detailed chemical composition (wt%) of SLMed IN718 alloys was measured for AsBuilt and heat-treated samples using the Positive Material Identification (PMI) tester, an X-ray fluorescence spectrometer (Oxford Instruments Handheld XRF - X-MET8000 Series Analyser). XRF is a rapid and non-destructive method of performing semi-quantitative chemical analysis on a wide range of components for material verification and identification purposes.

3.5.2. Tensile Testing

Tensile tests aimed to determine the yield strength, modulus of elasticity, ultimate tensile strength, uniform elongation, and total elongation. Tests were conducted at room temperature using a Zwick-Roell Z250 servo-hydraulic machine with a capacity of 250 kN in accordance with ASTM E8-M. An extensometer, as shown in Figure 3.11, was fitted to the machine. The tests were performed with a displacement control of 0.005 mm/s. The specimens were created following the guidelines of ASTM E8-16 and had a thickness of 6mm. To assess the repeatability of the SLM process, at least three samples were printed and tested for each set. The samples were tested in their AsBuilt surface condition, as shown in Figure 3.12.



Figure 3.11 Zwick-Roell Z250 tensile test machine


Figure 3.12 Specimens subjected to tensile test

3.5.3. Hardness Measurements

Vickers Microhardness measurements (HV) were conducted on all surfaces of the specimens after they were cleaned and polished. A load of 500 g and a loading time of 10 seconds were applied during testing. Hardness readings were taken at four designated test points (1, 2, 3, 4) on each surface of the specimen (A, B, C, D), considering both the longitudinal (X) and transverse (Y) directions. These test points were positioned at a distance of at least 2.5 and 3 times the indentation diagonal from the specimen contour and adjacent measurements respectively, as illustrated in Figure 3.13. The indentation images can be seen on Figure 3.14. The standard deviation was calculated based on the measurements taken, and the average hardness was determined by calculating the arithmetic mean of the obtained values.

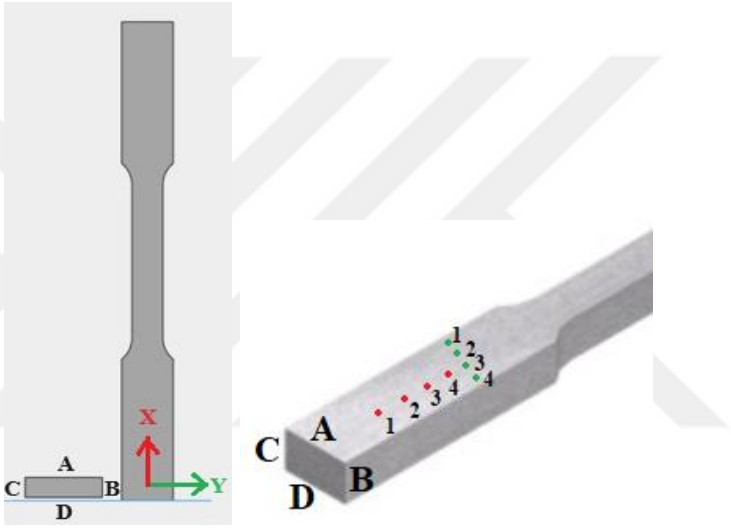


Figure 3.13 Surface codes and direction of hardness measuring lines

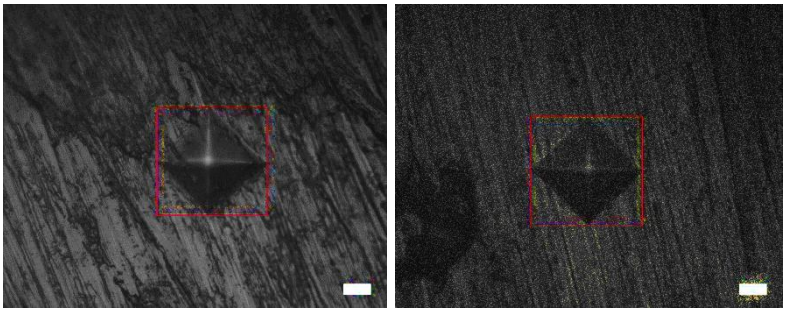


Figure 3.14 The indentation images

4. RESULTS AND DISCUSSION

SLMed IN718 AsBuilt, HA and NA heat-treated test specimens, built horizontally and vertically, subjected to XRF, tensile, and hardness tests. The results for each specimen were evaluated and compared with ER-IN718 and Wrought (Rw) IN718 data, as well as other results discussed in the literature.

Table 4.1 shows the powder characterization results obtained by Ermaksan. The particle size distribution, evaluated according to ASTM B214, indicates that only 2.1% of the particles have a size larger than 45 μm, while the majority, accounting for 97.9%, has a size of 45 μm or smaller. The particle size distribution based on ASTM B822, is provided with values for D10, D50, and D90 at 22, 33, and 44 μm, respectively. The total percentage of particles smaller than 45 μm is 3%. The flow rate was determined to be 3.1 seconds for 50g of powder, while the apparent density was measured at 4.59 g/cm^3. These measured values of powder properties conform to the relevant standards.

Table 4.1 Measured powder characterization

Description	**Measured**
Particle size distribution per ASTM B214	
Particle Size (μm)	% By mass
>45	2.1
≤45	97.9
Particle size distribution per ASTM B822	
D10	22 μm
D50	33 μm
D90	44 μm
<45 μm	3 %
Flow Rate ASTM B212 (Hall Flowmeter)	
Flow rate (sec. For 50g)	3.1
Apparent Density per ASTM B212	
Apparent Density (g/cm^3)	4.59

4.1. XRF Analysis

Table 4.2 and Figure 4.1 display the chemical composition of each specimen, expressed in weight percentages, as determined by the XRF test.

After homogenization annealing, the Nickel (Ni) content of the specimens produced in both horizontal and vertical building directions decreased, while the content of Chromium (Cr), Titanium (Ti), and Niobium (Nb) increased. The Ni ratio increased in both directions following the NA heat treatment, similar to the AsBuilt samples. Furthermore, the Cr ratio decreased while the Iron (Fe) ratio slightly increased compared to the samples that underwent HA. Additionally, the ratios of Cr, Ti, and Nb decreased. When comparing the AsBuilt specimens produced by SLM with the Rw IN718 and ER-IN718, it is evident that the specimens produced by SLM are consistent with

the Ermak. Additionally, the AsBuilt specimens closely approach the upper limit of the Rw IN718, with only a slightly higher Fe ratio.

Table 4.2 The chemical composition of the specimens with weight percentages

Specimen Name	Ni	Cr	Fe	Nb	Ti	Mo	Mn	Cu
H-AsB	52,85	19,48	18,14	4,91	1,25	2,98	0,29	0,11
H-HA	41,72	25,76	18,63	7,11	3,41	2,9	0,23	0,11
H-NA	51,88	15,69	19,85	6,22	2,77	3,27	0,11	0,11
V-AsB	52,56	19,75	18,15	4,93	2,94	1,18	0,3	0,09
V-HA	39,4	26,59	18,8	5,54	6,77	2,4	0,18	0,17
V-NA	47,18	21,05	20,34	5,43	2,57	3,18	0,03	0,12
Rw IN718 – (ASTM B637) (ASM, 2023)	50-55	17-21	17	4,75-5,5	0.65-1,15	2,80-3,3	0,35	0,3
Ermak A241-INC 718 (Ermaksan, 2023)	52,3	19,1	Balance	5,16	0,96	3,03	0,1	<0,1

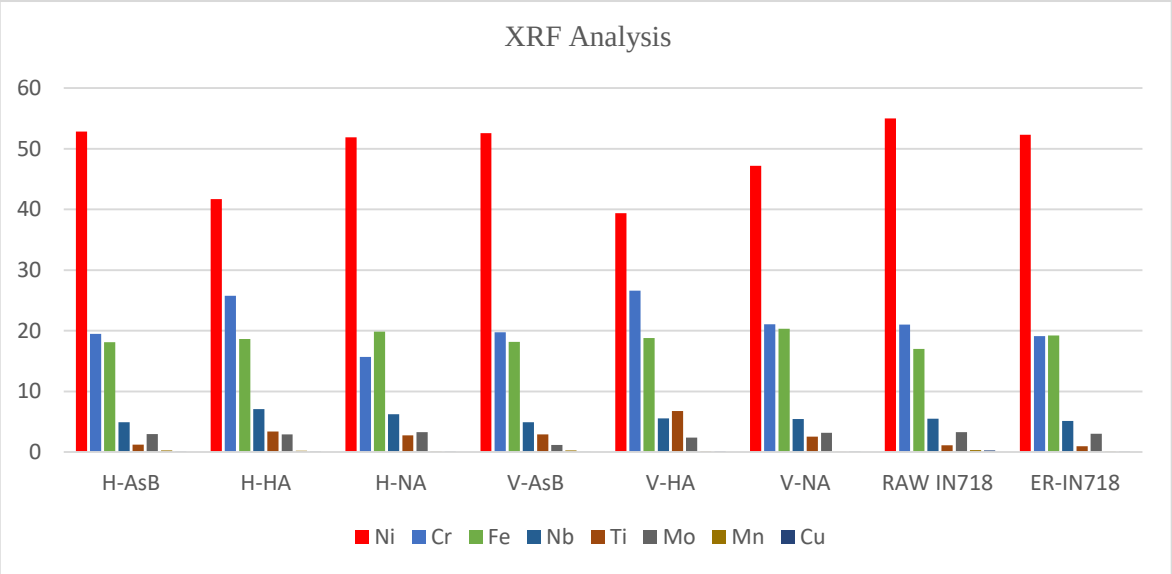


Figure 4.1 Results of XRF analysis

4.2. Tensile Tests

The specimens used in this study were designed in accordance with the ASTM tensile testing standard (ASTM E8-M, 2016). The results of the tensile test for each sample group were evaluated and compared based on the production directions using ER-IN718 and Rw IN718 data, as well as previous studies.

4.2.1. Horizontal Production Direction

By comparing the horizontally produced specimens based on the tensile test results, it is evident that the aged heat-treated specimen has the highest yield strength and tensile strength, measuring 1128 and 1200 MPa, respectively. Additionally, it is worth noting that the AsBuilt specimens have the highest elongation ratio. When compared to AsBuilt specimen (Figure 4.2), the HA (Figure 4.3) showed an increase of approximately 20% in yield stress and 17% in tensile stress,

but a decrease of approximately 6% in elongation. Similarly, the NA specimen (Figure 4.4) exhibited an increase of 44% in yield stress and 28% in tensile stress, but a decrease of 26% in elongation. All fractured horizontal specimens after tensile testing are shown in Figure 4.6.

Compared to Rw IN718 and HA heat treatment, the yield stress decreased by 14%, while the tensile stress decreased by 20% and the strain increased by 22%. The mechanical properties of the horizontally produced specimens are almost identical to those of Rw IN718. In comparison to ER-IN718, the yield stress of NA treated increased by 48%, the tensile stress increased by 15%, but the elongation decreased by 4%.

Compared to Li (2019) study, the NA specimen exhibited a 5% increase in yield strength but a 9% reduction in tensile strength (Li et al., 2019). Similarly, the Aged parts demonstrated a 9% decrease in yield strength and a 15% decrease in tensile strength compared to Aydinöz (2016) (Aydinöz et al., 2016).

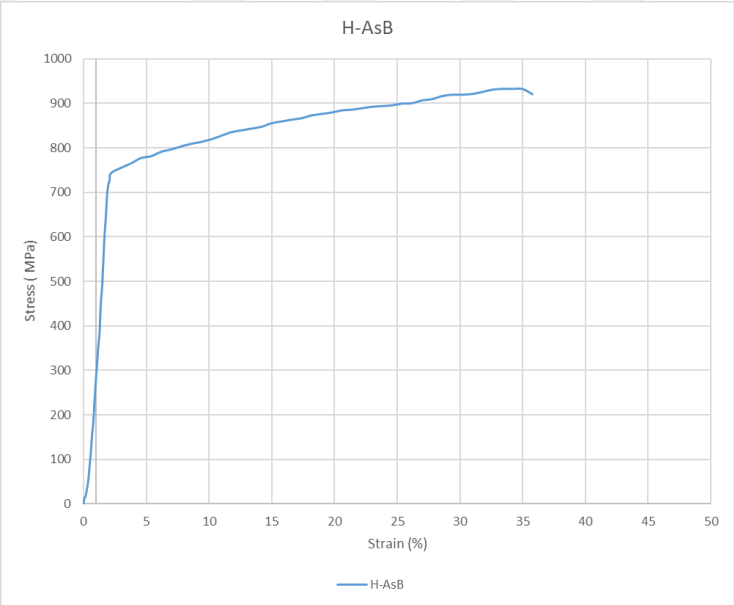


Figure 4.2 Stress-Strain curve of asbuilt state

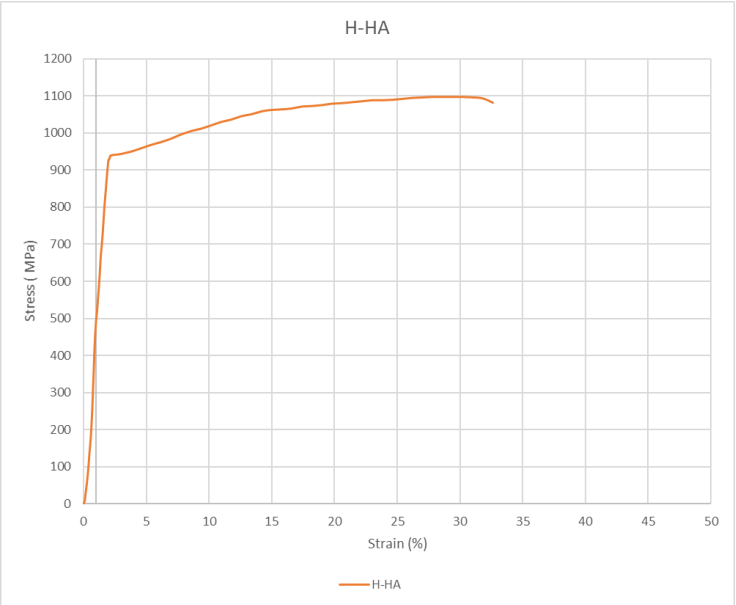


Figure 4.3 Stress-Strain curve of homogenized specimen

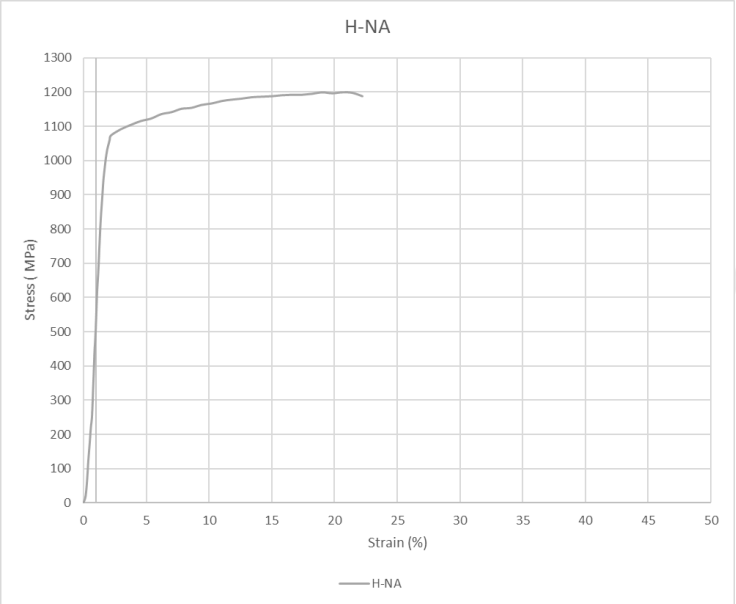


Figure 4.4 Stress-Strain curve of new-aged specimen

When comparing the tensile test results of SLMed IN 718 parts produced horizontally in the AsBuilt state and with the two heat treatments used to other studies (as shown in Figure 4.5), similar results were found in yield strength. This is because the identically produced specimens were subjected to a similar homogenisation annealing in most of the studies compared. The difference in tensile strength is due to the variation in the duration of the ageing heat treatment. The ageing process of the new heat treatment applied to the horizontally orientated IN718 specimens was faster and completed in one step compared to other studies. This is believed to be the main reason for the difference in tensile strength.

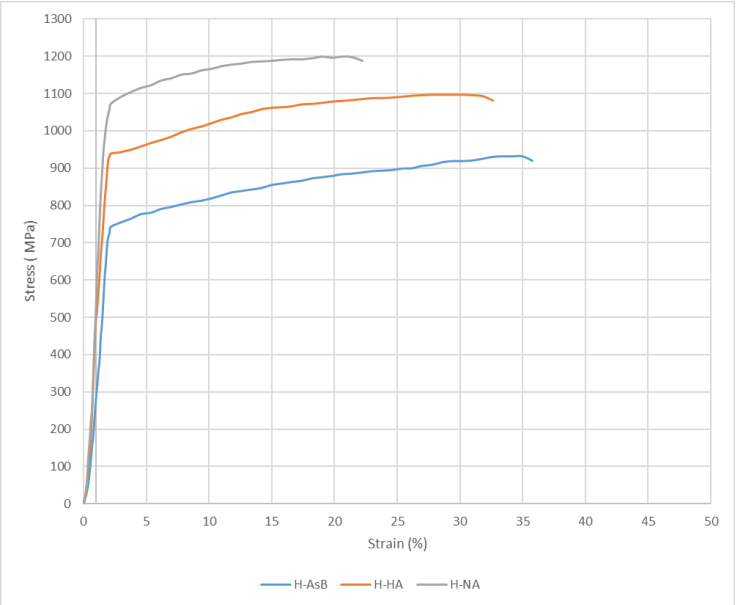


Figure 4.5 Stress-Strain curves of horizontally built specimens



Figure 4.6 Fractured specimens after tensile test

4.2.2. Vertical Production Direction

When the vertically produced specimens are compared after tensile tests, it is clear that the aged heat treated specimen shows the highest yield strength and tensile strength, measuring 950 and 1034 MPa, respectively. Also, the HA specimen (Figure 4.8) exhibits the highest elongation ratio. Compared to AsBuilt specimen (Figure 4.7), the NA specimen (Figure 4.9), yield stress increased approximately 46%, tensile stress increased approximately 27%, but elongation decreased 21%. For the HA specimen, in yield stress decreased of approximately 5%, in tensile stress increased 0.5%, and increased of approximately 11% in elongation. All fractured vertical specimens after tensile testing are shown in Figure 4.11.

Compared to Rw IN718 and HA heat treatment, the yield stress decreased by 43%, while the tensile stress decreased by approximately 40% but the strain increased by 62%. In comparison

to ER-IN718, the yield stress of HA treated decreased by approximately 16%, the tensile stress increased by 13%, but the elongation increased by 16%.

When comparing ER-IN718 and NA heat treatment, yield stress increased approximately 50%, tensile stress increased approximately 7%, and elongation decreased 5%.

Compared to the study of Popovich et al. the Homogenized specimen showed a 7% improvement in yield strength and a 7% decrease in tensile strength. The NA specimen showed a decrease of 8% in yield strength and a decrease of 10% in tensile strength (Popovich et al., 2017). Compared to the study of Chlebus et al. the NA specimen showed a decrease in yield strength of 11%, while the tensile strength showed a decrease of 21% (Chlebus et al., 2015).

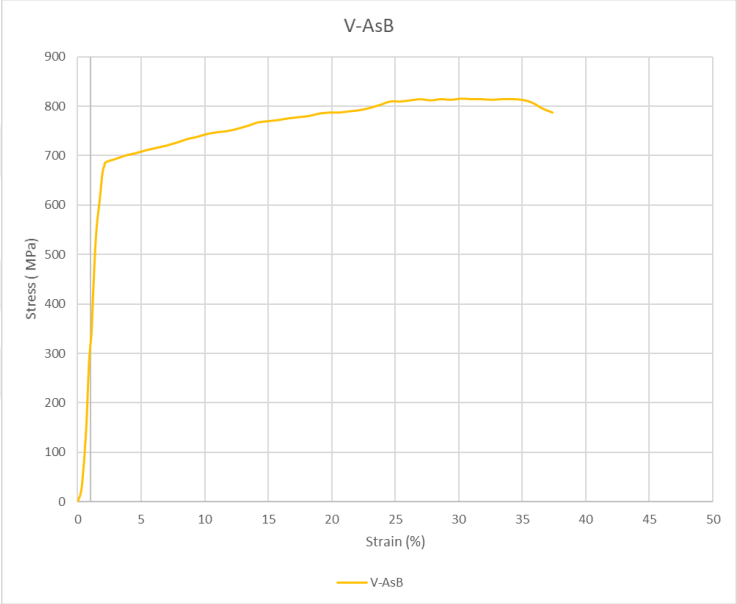


Figure 4.7 Stress-Strain curve of asbuilt state

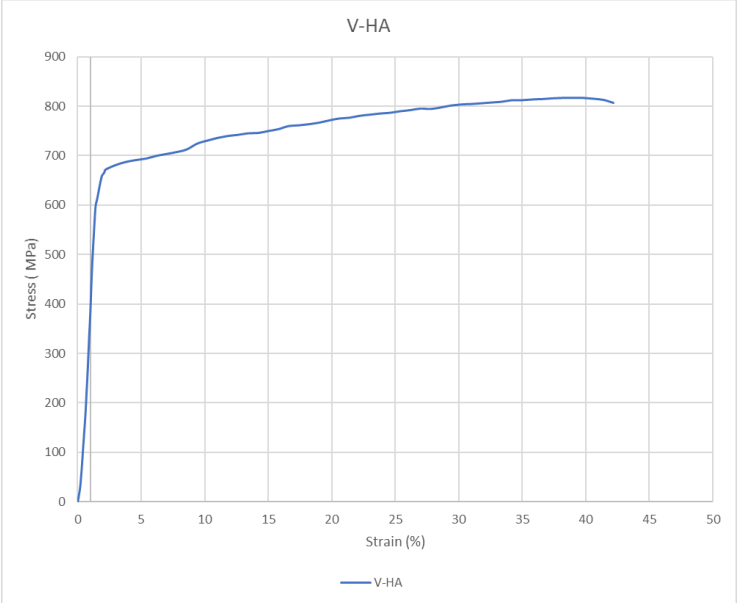


Figure 4.8 Stress-Strain curve of homogenized specimen

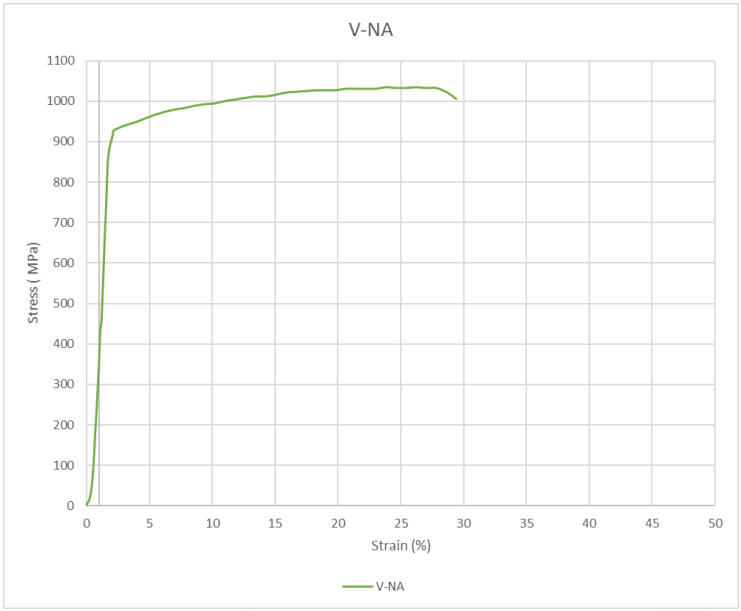


Figure 4.9 Stress-Strain curve of new-aging specimen

Comparing the results of the tensile tests performed on vertically produced SLMed IN 718 parts, it was observed that both yield strength and tensile strength exhibited similar results compared to the AsBuilt part and other related studies, as shown in Figure 4.10. This can be attributed to the fact that in most of these studies the specimens were manufactured in a similar manner and then subjected to a similar homogenisation annealing process. Furthermore, the aging process was faster compared to previous studies when compared to the new heat treatments applied to vertically oriented IN718 specimens. Moreover, this process was completed in a single step. Interestingly, the change in the duration of the aging heat treatment had minimal effect on the tensile strength. Consequently, it is assumed that the reduction of the aging heat treatment time does not significantly affect the tensile strength.

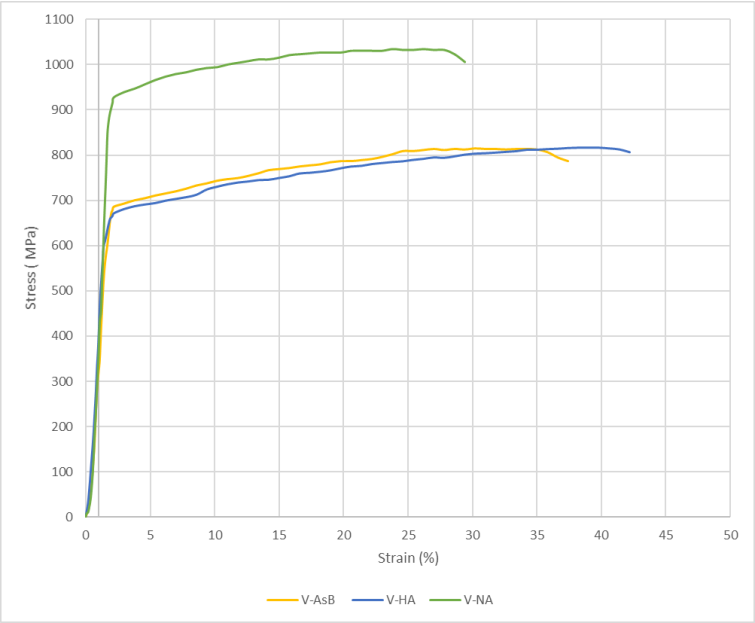


Figure 4.10 Stress-Strain curve of vertical specimens



Figure 4.11 Fractured specimens after tensile test

4.3. Evaluation of Hardness Measurements

The specimens were mechanically cleaned and polished prior to hardness testing and Vickers hardness values were measured using a 500g test weight. The results were compared with each other, Rw IN718, ER-IN718 and other previous work available in the literature. For the four surfaces shown as #A, #B, #C, #D, four hardness indentations shown as #1, #2, #3, #4 were measured and the average of the hardness values for each group was calculated (Figure 3.14). Here, X axis represents the building direction.

The hardness of the specimens produced in the horizontal direction of building decreased by 2% in the HA. On the other hand, the hardness of the aged increased by 8% compared to the AsBuilt state. In the vertical build direction, the homogenized specimens exhibited a 12% decrease in hardness, while the aged specimens demonstrated a 13% increase compared to the AsBuilt condition.

The hardness of IN718 specimens that were vertically produced and then aged was significantly higher than that of the specimens that were only homogenised. The aged specimens

had a hardness increase of 30% compared to the homogenised ones. This result was consistent for both production directions, and the aged specimens had the highest hardness values among all the materials tested, including ER-IN718 and Rw IN718.

The hardness values of the specimens can be compared based on their construction method (horizontal or vertical) and their treatment (AsBuilt, HA, and NA). The results show that the horizontal specimens have higher hardness than the vertical ones, except for V-NA. The treatment also affects the hardness, with AsBuilt specimens having higher hardness than heat-treated ones, and NA specimens having the highest hardness. The standard deviations of the hardness values are generally low, indicating consistent measurements within each group (Table 4.3.)

Table 4.3 Hardness measurements for surface #A on x-axis

A-x							
Specimen Name	**#1**	**#2**	**#3**	**#4**	**Max**	**Avg.**	**Std. Dev.**
H-AsB	396,8	404,5	426,2	396,8	426,2	406,0	13,9
H-HA	331,5	310,3	285,6	294,3	331,5	305,4	20,2
H-NA	361,4	365,8	314,7	325,7	365,8	341,9	25,5
V-AsB	324,8	364,7	353,8	339,3	364,7	345,6	17,4
V-HA	276,6	274,4	267,2	241,3	276,6	264,8	16,2
V-NA	331,5	368,1	366,9	359,2	368,1	356,4	17,1

For the horizontal specimens, the as-built specimen had the highest maximum and average hardness, 411.1 and 390.9, followed by the H-NA and the H-HA. For the vertical specimens, the as-built (V-AsB) specimen also had the highest maximum and average hardness, 289.5 and 271.1, followed by the V-NA and the V-HA. The hardness values of the horizontal specimens were generally higher than those of the vertical, except for the heat-treated, which had similar hardness values in both orientations (Table 4.4).

Table 4.4 Hardness measurements for surface #A on Y-axis

A-y							
Specimen Name	**#1**	**#2**	**#3**	**#4**	**Max**	**Avg.**	**Std. Dev.**
H-AsB	411,1	371,5	388,1	393	411,1	390,9	16,3
H-HA	291,1	285,6	261	303,4	303,4	285,3	17,8
H-NA	341,3	378,5	351,7	333,4	378,5	351,2	19,7
V-AsB	334,4	343,4	340,3	372,6	372,6	347,7	17
V-HA	280,3	259,7	255,1	289,5	289,5	271,1	16,4
V-NA	315,6	304,3	334,4	366,9	366,9	330,3	27,4

The hardness measurements for surface #B along the x-axis revealed significant variations among the specimens depending on their orientation and treatment. The horizontal specimens (H-AsB, H-HA, and H-NA) exhibited higher hardness values than the vertical specimens (V-AsB, V-HA, and V-NA), indicating a possible effect of gravity on the microstructure formation during the AM process. The homogenization annealed specimens (H-HA and V-HA) showed lower hardness than the as-built, suggesting a softening effect of the heat treatment. The Aged specimens (H-NA and V-NA) displayed higher hardness than the homogenizationed, indicating a hardening effect of the aging process (Table 4.5).

Table 4.5 Hardness measurements for surface #B on x-axis

B-x							
Specimen Name	**#1**	**#2**	**#3**	**#4**	**Max**	**Avg.**	**Std. Dev.**
H-AsB	386,9	383,2	365,8	374,9	386,9	377,7	9,4
H-HA	413,8	422	483,5	390,5	483,5	427,4	39,7
H-NA	426,2	480,1	459	371,5	480,1	434,2	47,3
V-AsB	340,3	344,4	335,4	334,4	344,4	338,6	4,6
V-HA	272,9	285,6	315,6	292,7	315,6	291,7	17,9
V-NA	401,9	363,6	448,1	420,6	448,1	408,5	35,5

The hardness measurements for surface #B on y axis show significant variations (Table 4.6). The highest hardness was obtained by H-NA with 486.9, followed by V-NA with 499.2. The lowest hardness was obtained by V-HA with 251.8, followed by V-AsB with 330.5. The average hardness also reflects this trend, with H-NA and V-NA having the highest averages of 472 and

436.3 respectively, and V-HA and V-AsB having the lowest averages of 287.8 and 333.8 respectively. These results suggest that the hardness of the specimens depends on both the heat treatment and the alloy composition.

Table 4.6 Hardness measurements for surface #B on y-axis

B-y							
Specimen Name	**#1**	**#2**	**#3**	**#4**	**Max**	**Avg.**	**Std. Dev.**
H-AsB	357	353,8	338,3	346,4	357	348,9	8,3
H-HA	430,4	376,1	394,3	440,6	440,6	410,4	30,3
H-NA	486,9	470,2	475,1	455,8	486,9	472	12,9
V-AsB	330,5	343,4	343,4	341,3	347,5	333,8	9,3
V-HA	251,8	287,2	286,4	325,7	325,7	287,8	30,2
V-NA	423,4	451,2	499,2	371,5	499,2	436,3	53,4

From the table 4.7, we can observe that AsB has the highest maximum and average hardness values in both building directions, followed by NA and then HA. The highest maximum hardness is 426.2 for H-AsB, and the lowest is 267.2 for V-HA. We can also notice that the hardness values in Vertical building directions are lower than the horizontal for all specimens. This indicates that the vertical building direction is more sensitive to the microstructure and composition of the specimens than the horizontal. Also, it indicates that AsB is the most resistant to indentation among the other specimens

Table 4.7 Hardness measurements for surface #C on x-axis

C-x							
Specimen Name	**#1**	**#2**	**#3**	**#4**	**Max**	**Avg.**	**Std. Dev.**
H-AsB	374,9	399,3	426,2	386,9	426,2	396,8	22
H-HA	291,1	304,3	275,1	322,9	322,9	298,4	20,3
H-NA	347,5	344,4	360,3	343,4	360,3	348,9	7,8
V-AsB	327,6	328,6	347,5	331,5	347,5	333,8	9,3
V-HA	276,6	275,1	284,8	267,2	284,8	275,9	7,2
V-NA	342,3	287,2	363,6	322	363,6	328,8	32,5

The hardness measurements for surface #C on y axis are shown in Table 4.8. It can be observed that the maximum and average hardness for H-AsB are the highest among all specimens, indicating that the as-built condition has the highest resistance to plastic deformation. The H-HA specimen has the lowest hardness, suggesting that the homogenization annealing and aging process reduces the hardness of the material. The H-NA specimen does not have any data available, due to experimental errors or difficulties in measuring the hardness of the aged layer.

Table 4.8 Hardness measurements for surface #C on y-axis

C-y							
Specimen Name	**#1**	**#2**	**#3**	**#4**	**Max**	**Avg.**	**Std. Dev.**
H-AsB	361,4	390,5	386,9	396,8	396,8	383,9	15,6
H-HA	282,5	300	305,1	292,7	305,1	295,1	9,8
H-NA	-	-	-	-	-	-	-
V-AsB	322,9	330,5	332,4	328,6	332,4	328,6	4,1
V-HA	270	276,6	283,3	256,4	283,3	271,6	11,5
V-NA	342,3	341,3	305,1	349,6	349,6	334,6	20

From the Table 4.9, we can observe that the hardness varies significantly among all the specimens, especially for the horizontal specimens (H-AsB, H-HA, and H-NA). The highest hardness value is obtained by H-HA with a maximum of 485.2 and an average of 459.5, while the lowest hardness is obtained by V-AsB with a maximum of 325.7 and an average of 318.3. The hardness also shows a large variation within each specimen, indicating that the surface #D is not uniform in hardness across the x axis. The results also show that the horizontal specimens have higher hardness than the vertical for all treatments, except for V-NA, which has a higher maximum and average than H-NA. This suggests that the building direction of the specimen affects the hardness of surface #D on x axis.

Table 4.9 Hardness measurements for surface #D on x-axis

D-x							
Specimen Name	**#1**	**#2**	**#3**	**#4**	**Max**	**Avg.**	**Std. Dev.**
H-AsB	366,9	340,3	345,4	343,4	366,9	349	12,1
H-HA	439,1	445,1	485,2	468,6	485,2	459,5	21,3
H-NA	360,3	371,5	401,9	354,9	401,9	372,1	21
V-AsB	321,1	322	325,7	304,3	325,7	318,3	9,5
V-HA	321,1	313,8	320,2	324,08	324,8	320	4,6
V-NA	393,9	420,6	399,3	393	493,9	426,7	46,3

In this section, we analyzed the hardness measurements for surface #D on y axis. From the Table 4.10, we can observe that the heat-treated specimens have higher hardness than the as-built specimens, and the NA specimens have higher hardness than the HA. This indicates that the heat treatment processes enhance the hardness of the surface #D on y axis. The lowest hardness value is observed for V-AsB, followed by H-AsB and H-NA. We can also observe that the vertically built specimens have lower hardness than the horizontally, except for V-NA which has slightly higher hardness than H-NA. This suggests that the vertically buildings process reduces the hardness of the surface #D on y axis, unless it is combined with NA. We can also notice that aging has a positive effect on the hardness of both NA and vertically built specimens, while as-built have lower hardness than aged one.

Table 4.10 Hardness measurements for surface #A on Y-axis

D-y							
Specimen Name	**#1**	**#2**	**#3**	**#4**	**Max**	**Avg.**	**Std. Dev.**
H-AsB	340,3	364,7	353,8	344,4	364,7	350,8	10,9
H-HA	384,4	490,4	457,4	490,4	490,4	455,6	50
H-NA	398,1	395,5	380,8	369,2	398,1	385,9	13,5
V-AsB	315,6	327,6	319,2	322	327,6	321,1	5,1
V-HA	352,7	324,8	420,6	328,6	420,6	356,7	44,4
V-NA	395,5	423,4	422	372,6	423,4	403,4	24,2

Figure 4.12 presents the average vickers hardness for different specimens. The results showed that the H-AsB specimen had the highest hardness among the horizontally building

direction group, with an average value of approximately 350 Vickers hardness. The H-HA specimen had a slightly lower hardness, around 325, while the H-NA specimen had the lowest hardness of all, about 275. This suggests that AsBuilt condition increases the hardness of the material, while NA decreases it. The V-AsB specimen had a lower hardness than the H-AsB specimen, with an average value of approximately 300 Vickers hardness. The V-HA specimen had a similar hardness to the H-HA specimen, around 325, while the V-NA specimen had the highest hardness among the vertically building direction group, close to 400. This indicates that vertically building enhances the hardness of NA, but reduces the hardness of AsBuilt specimen.

In conclusion, the findings demonstrate a statistically significant influence of both building direction and heat treatment on the hardness of the material. AsBuilt specimens exhibited lower average hardness compared to their counterparts with homogenization Annealing treatment. Additionally, horizontally built specimens exhibited higher average hardness compared to vertically built specimens. These observations suggest that the manufacturing process parameters, including building direction and heat treatment, play a crucial role in tailoring the material's mechanical properties.

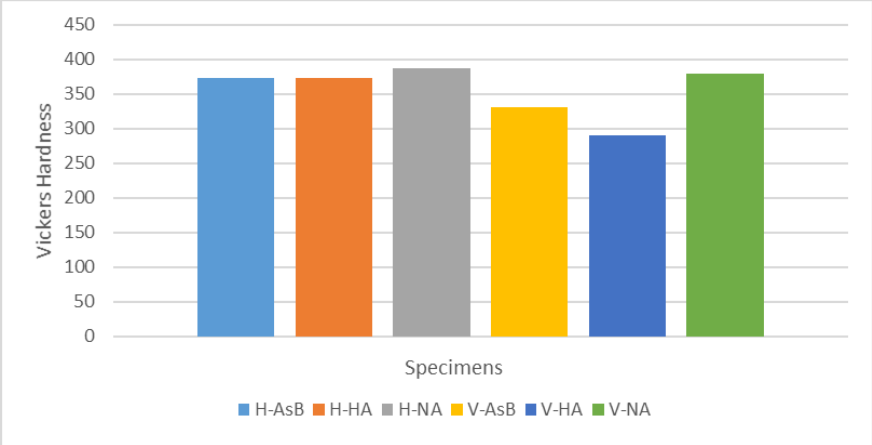


Figure 4.12 Average vickers hardnesses

4.3.1. The Impact of Post Heat Treatments on the Mechanical Characteristics

XRF analysis of IN718 samples produced by SLM revealed variations in elemental composition. These variations were observed both in the AsBuilt state and in samples subjected to subsequent homogenization annealing and a novel ageing heat treatment. Notably, the Ni concentration remained the highest across all examined conditions. Conversely, HA yielded the lowest Ni and highest Cr ratios. These observations suggest preferential dissolution of Ni into the Inconel matrix during SLM processing, potentially leading to enrichment of Cr at grain boundaries due to homogenization heat treatment.

Analysis of the IN718 material's Time-Temperature-Transformation (TTT) diagram suggests that holding temperatures exceeding 1040°C will facilitate an enhanced dissolution of the δ phase.

This phenomenon was observed in specimens subjected to a heat treatment regime of 1170 °C for 2 hours, exhibiting a related decrease in material hardness, increase in elongation rate, and reduction in yield strength as the δ phase dissolved. This transformation was accompanied by the evolution of the matrix microstructure and carbide formation. Notably, the accompanying recrystallization process effectively eliminates residual stresses introduced during the SLM process, leading to an overall improvement in material mechanical properties. However, it is crucial to acknowledge that recrystallized structures can experience a decline in strength due to the presence of larger grains compared to their non-recrystallized counterparts.

In the context of this investigation, the absence of a controlled environment during the heat treatment process leads to anticipated surface oxidation and carbide formation. Subsequent XRF analysis of the aged specimens revealed a notable increase in the Ni content relative to the Homogenized group, accompanied by a concomitant decrease in the Cr content.

Among AsBuilt specimens, H-AsB demonstrated the highest tensile and yield strength, while V-AsB exhibited the greatest elongation. This finding suggests a potential advantage for the horizontal building direction regarding strength in the AsBuilt state. Following homogenization annealing, V-HA specimens displayed the lowest tensile and yield strength among the homogenized group, while H-HA exhibited the least elongation. This observation suggests a potential detrimental effect of the vertical building direction on material properties after homogenization annealing. All aged specimens exhibited higher tensile and yield strength compared to their AsBuilt or homogenized counterparts. However, elongation was generally lower in the aged group. Interestingly, H-NA specimens retained the highest tensile and yield strength within the aged group, while V-NA maintained the highest elongation (Table 4.11.)

An initial evaluation of the horizontal specimens revealed the lowest tensile strength (933 MPa) and highest elongation (32.5%) for the AsBuilt condition. Subsequent HA treatment resulted in a significant increase in tensile strength (1095 MPa), while maintaining a substantial elongation level. Further NA treatment exhibited the highest observed tensile strength (1200 MPa), albeit accompanied by a 25% reduction in elongation at break. Similar to the horizontal samples, the AsBuilt vertical specimens displayed the lowest initial tensile strength (813 MPa) with the highest elongation (36%). HA treatment produced a minor increase in tensile strength (817 MPa) but interestingly yielded an augmented elongation (12%). The NA treatment ultimately yielded the highest tensile strength (1034 MPa) within the vertical group, coupled with a notable 25% decrease in elongation compared to homogenized specimens. There seems to be no significant difference in tensile strength or elongation between horizontally and vertically built specimens within the same treatment group (AsBuilt, Homogenized, Aged). This suggests that the building direction of the specimen during testing does not have a major impact on the results for Inconel 718 in this study. Heat treatment significantly affects the tensile properties of Inconel 718. New Aging generally leads to the highest tensile strength and yield strength, followed by homogenization and then

AsBuilt condition. However, NA also tends to decrease elongation compared to AsBuilt or homogenized specimens.

The tensile strength and yield strength for most specimens are higher than the typical range reported for Inconel 718 (1034 MPa to 1379 MPa for tensile strength and 724 MPa to 1103 MPa for yield strength). This could be due to differences in material composition, processing methods, or testing conditions.

Table 4.11 Tensile test results

Specimen Name		Orientation	Heat Treatment	Yield Strength MPa	Tensile Strength MPa	Elongation %
1	H-AsB	Horizontal	AsBuilt	779	933,63	32,5
2	H-HA	Horizontal	Homogenized	938	1095,5	30,5
3	H-NA	Horizontal	Aged	1128	1200,88	24
4	V-AsB	Vertical	AsBuilt	649	813,7	36
5	V-HA	Vertical	Homogenized	618	817	40,5
6	V-NA	Vertical	Aged	950	1034,37	28,5
7	(Li et al., 2019)	Horizontal	Aged	1070	1320	24
8	(Chlebus et al., 2015)	Vertical	Aged	1074	1320	19
9	(Popovich et al., 2017)	Vertical	Homogenized	574	873	13
10		Vertical	Aged	1041	1154	7
11	(Aydinöz et al., 2016)	Horizontal	Homogenized	535	870	34,5
12		Horizontal	Aged	1240	1400	9
13	Rw IN718 – (ASTM B637) (ASM, 2023)	-		1100	1375	25
14	Ermak A241-INC 718 (Ermaksan, 2023)	Vertical	AsBuilt	636	971	30
15		Horizontal	AsBuilt	758	1040	25

Among the AsBuilt specimens, H-AsB had the highest average hardness. This indicates an advantage for the horizontal built direction in terms of hardness in the AsBuilt state. After homogenization annealing, V-HA specimens exhibited the lowest average hardness among the homogenized group, while H-HA exhibited the highest average hardness. This observation suggests that the vertical built direction has a potentially detrimental effect on the material properties after homogenization annealing. As can be seen in Table 4.12, all aged specimens exhibited higher average hardness compared to their as-built or homogenized counterparts. H-NA exhibited the highest average hardness of all groups.

Hardness evaluation of the specimens showed that the AsBuilt state exhibited a hardness in the mid-range (375 HV) among the horizontal specimens. The subsequent HA treatment caused a

decrease in hardness, with the lowest average hardness (367 HV) exhibited by H-HA. H-NA exhibited the highest average hardness measured among all groups (386 HV) with the subsequent NA treatment. Similar to the horizontal specimens, the AsBuilt state showed a hardness in the mid-range among the vertical specimens (333 HV). In hardness with HA treatment (292 HV) V-HA showed the lowest average hardness among all groups. H-NA had the highest hardness (378 HV) among the vertical group as a result of the NA treatment. Heat treatment significantly affects the hardness properties of Inconel 718. New Aging usually leads to the highest hardness, followed by AsBuilt and Homogenization. However, NA also tends to increase hardness. Also, horizontal specimens were characterized by slightly higher hardness than vertical specimens.

Table 4.12 Hardness test results

	Specimen Name	**Orientation**	**Heat Treatment**	**Vickers HV (Avg.)**
1	H-AsB	Horizontal	AsBuilt	375,51
2	H-HA	Horizontal	Homogenized	367,14
3	H-NA	Horizontal	Aged	386,6
4	V-AsB	Vertical	AsBuilt	333,44
5	V-HA	Vertical	Homogenized	292,46
6	V-NA	Vertical	Aged	378,13
7	(Chlebus et al., 2015)	Vertical	Aged	463
8	(Popovich et al., 2017)	Vertical	Homogenized	370
9		Vertical	Aged	478
10	(Aydinöz et al., 2016)	Horizontal	Homogenized	280
11		Horizontal	Aged	215
12	Rw IN718 – (ASTM B637) (ASM, 2023)	-		340
13	Ermak A241-INC 718 (Ermaksan, 2023)	Vertical	AsBuilt	302
14		Horizontal	AsBuilt	277

Compared to other studies, the hardness values are within the typical ranges reported for Inconel 718 (478 HV to 277 HV). This range may be due to differences in material composition, processing methods, or test conditions.

5. CONCLUSION AND FUTURE STUDIES

5.1. Conclusion

This study investigates the mechanical properties, including tensile strength and hardness, of IN718 parts fabricated using SLM. The study takes into account the direction of production and the heat treatments applied, such as homogenization annealing and new aging. The objective is to collect valuable information to enhance the production process and attain the intended mechanical properties for the high-temperature resistance component.

The tensile strength of horizontally built specimens was significantly improved by the aging heat treatment, whereas the elongation of vertically built specimens was improved by the annealing heat treatment. The tests showed that heat treatment improved the mechanical properties of SLMed IN718, making it suitable for high temperature and strength applications. The new heat treatment process completed aging faster and in a single step compared to previous studies, which is believed to be the main reason for the improved mechanical properties. The results can be liste as;

- After the NA heat treatment, the Ni ratio in the internal structures of the samples increased compared to those subjected to homogenization annealing and reached a ratio similar to the As-Built samples in both directions.
- When comparing horizontally produced samples based on the results of the tensile test, it can be seen that the aged ones have the highest yield and tensile strength, measuring 1128 and 1200 MPa, respectively. When compared to the AsBuilt samples, the NA sample exhibited an increase of approximately 44% in yield stress and 28% in tensile stress.
- Compared to Rw IN718 and HA heat treatment, the yield stress decreased by 14%, while the tensile stress decreased by 20% and the strain increased by 22%. The mechanical properties of the horizontally produced specimens are almost identical to those of Rw IN718. In comparison to ER-IN718, the yield stress of NA treated increased by 48%, the tensile stress increased by 15%, but the elongation decreased by 4%.
- When comparing the vertically produced specimens after tensile tests, it is evident that the aged heat-treated specimen has the highest yield strength and tensile strength, measuring 950 and 1034 MPa, respectively. Additionally, the HA specimen exhibits the highest elongation ratio. Compared to the AsBuilt state, the yield stress of the NA increased by 46% and the tensile stress increased by 27%.
- Compared to Rw IN718 and HA heat treatment, the yield stress decreased by 43%, while the tensile stress decreased by 40%, but the strain increased by 62%. In

comparison to ER-IN718, the yield stress of HA treated decreased by 16%, the tensile stress increased by 13%, but the elongation increased by 16%. When comparing ER-IN718 and NA heat treatment, the yield stress increased by 50%, the tensile stress increased by 7%, and the elongation decreased by 5%.

- The hardness of H-AsB was the highest among the AsBuilt specimens, indicating that the horizontal built direction had an advantage in the AsBuilt state. The hardness of V-HA was the lowest among the homogenized specimens, while H-HA had the highest hardness, suggesting that the vertical built direction had a negative effect on the material properties after HA treatment.
- The hardness of all aged specimens was higher than their as-built or homogenized counterparts, with H-NA having the highest average hardness of all groups. The AsBuilt state had a medium hardness among both horizontal and vertical specimens, with 375 HV and 333 HV respectively.
- The HA treatment caused a decrease in hardness for both horizontal and verticallly built specimens, with V-HA having the lowest hardness of all groups (292 HV). The NA treatment increased the hardness for both horizontal and vertical direction, with H-NA having the highest hardness of all groups (386 HV).
- The heat treatment had a significant impact on the hardness properties of Inconel 718. The order of hardness from highest to lowest was NA, AsBuilt, and HA. The horizontal specimens also had slightly higher hardness than the vertical specimens.

In conclusion, this study has investigated the mechanical properties of SLMed IN718 parts, focusing on tensile strength and hardness, considering the direction of production and various heat treatments. The findings reveal that the aging heat treatment significantly enhances the tensile strength of horizontally built specimens, while the annealing heat treatment improves the elongation of vertically built specimens. The new aging process proves to be efficient, accomplishing faster and single-step aging, leading to notable improvements in mechanical properties. The study highlights the impact of heat treatments on internal structures, yielding increased Ni ratios and improved mechanical characteristics. The detailed comparison of horizontally and vertically produced specimens, along with various heat treatments, provides valuable insights for optimizing the production process to achieve desired mechanical properties for high-temperature resistance components. Overall, the results contribute to advancing the understanding and application of SLMed IN718 in high-stress and high-temperature environments, demonstrating the significance of tailored heat treatments for superior material performance.

5.2. Future Studies

This study examines a novel aging heat treatment process that aims to improve the mechanical properties of SLMed IN718 specimens. The mechanical properties were assessed through XRF, tensile, and hardness tests. The specimens were produced and analyzed in both horizontal and vertical building directions using identical manufacturing parameters. Further studies should be conducted to better understand the behaviour of the SLMed IN718 in high temperature environments. These studies may include:

- The examination of samples produced in different building directions and angles, taking into account various production parameters and the intended use of the parts.
- In order to obtain the required mechanical properties, it may be necessary to apply different heat treatments at different temperatures and durations instead of a single-stage ageing heat treatment.
- The mechanical tests were conducted at room temperature. It may be beneficial to perform these tests at higher temperatures, specifically between 550◦C-650◦C, to determine the suitability of the SLM component at its high service temperature.
- To comprehend the relationship between properties-processing-microstructure, the change in the microstructure of fractured specimens before and after heat treatment can be analyzed through Scanning Electron Microscopy (SEM).
- Fatigue testing is essential for evaluating resistance of material to cyclic loading. It provides crucial data for optimizing SLM process parameters and ensuring the structural integrity and longevity of components subjected to repetitive loading conditions.
- Creep tests are useful for understanding the time-dependent deformation of IN718 under constant load and elevated temperatures. They can help predict the material's behaviour over extended periods.
- Corrosion and oxidation resistance is essential to maintain the structural integrity, reliability and durability of components over time, especially in applications where exposure to corrosive substances, high temperatures and aggressive environmental conditions is common. Corrosion and oxidation characteristics for such applications can be analysed in detail.

REFERENCES

AMS, (2005). AMS 2774A. Heat treatment: wrought nickel alloy and cobalt alloy parts.

Alghamdi, S., John, S., Roy Choudhury, N., and Dutta, N. (2021). Additive Manufacturing of Polymer Materials: Progress, Promise and Challenges. Polymers. 13.

Amato, K., Gaytan, S., Murr, L., Martinez, E., Shindo, P., Hernandez, J., Medina, F. (2012). Microstructures and mechanical behavior of Inconel 718 fabricated by selective laser melting, Acta Mater. 60 (5) 2229–2239.

Anonymous 1. (2024). Wikipedia. Retrieved from Wikipedia: https://en.wikipedia.org/wiki/Superalloy#/media/File:Ni3Nb_Body_Centered_Tetragonal.JPG [accessed: 01.01.2024].

Arunachalam, R., Mannan, M., and Spowage, A. (2004). Residual stress and surface roughness when facing age hardened Inconel 718 with CBN and ceramic cutting tools. International Journal of Machine Tools and Manufacture, 44(9), 879-887.

ASM. (2023). Special Metals Inconel® Alloy 718. Retrieved from Aerospace Specisication Metals Inc.: https://asm.matweb.com/search/SpecificMaterial.asp?bassnum=NINC34 [accessed: 11.12.2023].

ASTM. (2016). ASTM E8-E8M-2016a.pdf. International.

ASTM F3055−14a, (2014). Standard Specification for Additive Manufacturing Nickel Alloy (UNS N07718) with Powder Bed Fusion, ASTM Int.

Aydinöz , M., Brenne, F., Schaper, M., Schaak, C., Tillmann, W., Nellesen, J., and Niendorf, T. (2016). On the microstructural and mechanical properties of post-treated additively manufactured Inconel 718 superalloy under quasi-static and cyclic loading,. Mater. Sci. Eng. A 669, 246–258.

Bhattacharya, S. J. (1983). Wear Mechanisms of Syalon Ceramic Tools when Machining Nickel-Based Material. Metals Technology, 482-483.

Candioto, K., Caliari, F., Reis, D., Couto, A., and Nunes, C. (2015). Characterization of the superalloy Inconel 718 after double aging heat treatment, Advanced Structured Materials, Springer. vol 70. pp. 293–300.

Chamanfar, A., et al. (2013). Microstructural characteristics of forged and heat treated Inconel-718 disks. Materials & Design (1980-2015), 52: 791-800.

Chlebus, E., Gruber, K., Kuźnicka, B., Kurzac, J., and Kurzynowski, T. (2015). Effect of heat treatment on the microstructure and mechanical properties of Inconel 718 processed by selective laser melting, Mater. Sci. Eng. A 639, 647–655.

Choi, J.P. et al. (2017). Densification and microstructural investigation of Inconel 718 parts fabricated by selective laser melting. Powder Technology. 310: p. 60-66.

Coromant. (2023). Heat resistant super alloys. Retrieved from Sandvik Coromant: https://www.sandvik.coromant.com/en-gb/industry-solutions/aerospace/hrsa [accessed: 11.12.2023].

Davis, J. R. (2000). ASM Speciality Handbook: Nickel, Cobalt and their alloys. USA.

Dawood , N. M., and Salim, A. M. (2021). A Review on Characterization, Classifications, and Applications of Super Alloys. Journal of University of Babylon for Engineering Sciences, Vol. (29), No. (1), 53-62.

Deng, D., Peng, R., Brodin, H., and Moverare, J. (2018). Microstructure and mechanical properties of Inconel 718 produced by selective laser melting: Sample orientation dependence and effects of post heat treatments, Mater. Sci. Eng.: A 713, 294–306.

Donachie, M. J. (2000). Superalloys: A Technical Guide (2nd Edition). ASM International.

Ergene, B. (2022). Simulation of the production of Inconel 718 and Ti6Al4V biomedical parts with different relative densities by selective laser melting (SLM) method. J. Facul. Eng. Architect. Gazi Univ. 37. https://doi.org/10.17341/gazimmfd.934143.

Ermaksan. (2023). ERMAK A241-INC 718 - Ermaksan - www.ermaksan.com.tr. Bursa, Nilüfer, Turkey.

Ermaksan. (2023). INC 718. Retrieved from Ermaksan Additive: https://www.ermaksanadditive.com/tr-TR/toz-cesitleri/inc-718 [accessed: 10.01.2024].

Frazier, W. (2014). Metal additive manufacturing: a review. Journal of Materials Engineering and Performance. 23(6), 1917-1928.

Garcia, C. et al. (1992). Thermomechanical processing and continuous cooling transformation behavior of IN-718. in Proc. Conf. Superalloys.

Gibson, I., Rosen, D. W., and Stucker, B. (2015). Additive Manufacturing Technologies. 2nd. New York, USA. Springer.

Greene, G., and Finfrock, C. (2001). Oxidation of Inconel 718 in Air at High Temperatures. Oxidation of Metals 55, 505–521. https://doi.org/10.1023/A:1010359815550.

Gu, D., and Jia, Q. (2014). Selective laser melting additive manufacturing of Inconel 718 superalloy parts: Densification, microstructure, and properties, Journal of Alloys and Compounds, Volume 585, Pages 713-721, ISSN 0925-8388.

Guo, N., and Leu, M. (2013). Additive manufacturing: technology, applications and research needs. Front. Mech. Eng. 8, 215–243. https://doi.org/10.1007/s11465-013-0248-8.

Hosseini, E., and Popovich, V. (2019). A review of mechanical properties of additively manufactured inconel 718. Additive Manufacturing, 30.

Huang , W., Yang, J., Yang , H., Jing, G., Wang, Z., and Zeng , X. (2019). Heat treatment of Inconel 718 produced by selective laser melting: microstructure and mechanical properties. Mater. Sci. Eng. A-Struct. Mater. Prop. Microstruct. Process;750:98–107.

Huang, X., Chaturvedi, M., and Richards, N. (1996). Effect of homogenization heat treatment on the microstructure and heat-affected zone microfissuring in welded cast alloy 718. Metallurgical and materials Transactions A. 27(3): 785-790.

Hunt R.C., Gazella R.M., Polanka M.D., Kemnitz R., Eckley C.C., Sexton B.M., Sebastian J.R., . (2022). Testing and Characterization of Additive and Traditionally Manufactured Inconel 718 in a Combustion Materials Test Facility.

Jia, Q., and Gu, D. (2014). Selective laser melting additive manufacturing of Inconel 718 superalloy parts: Densification, microstructure and properties. Journal of Alloys and Compounds, 585: p. 713-721.

Jiang, J., Gu, H., Li, B., Zhang, J., and Gu, Y. (2024). Effect of Solution Treatment on Mechanical Properties of Inconel 718 Alloy Formed by SLM. Journal of Physics: Conference Series.

Kim, H. et al. (1997). Effect of heat treatment on apatite-forming ability of Ti metal induced by alkali treatment. Journal of Materials Science: Materials in Medicine. 8(6): p. 341-347.

Klopp, W. D. (1995). Nickel Base Alloys:IN-718. In Aerospace Structural Metals Handbook. USA.

Konečná , R., and Nicoletto, G. (2019). On the link between as-built surface quality and fatigue behavior of additively manufactured inconel 718. International Conference Materials.

Korkmaz, M., E. Yasar, N., and Günay, M. (2020, Vol. 23). Numerical and experimental investigation of cutting forces in turning of Nimonic 80A superalloy. Eng. Sci. Technol. Int. J., pp. 664-673.

Kumar, L., Pandey, P., and Wimpenny, D. (2018). 3D Printing and Additive Manufacturing Technologies. Springer, Singapore.

Kuo, C., Yang, Y., Bor, H., Wei, C., and Tai, C. (2009). Aging effects on the microstructure and creep behavior of Inconel 718 superalloy, Mater. Sci. Eng. A. 510–511.

Kuo, C.M., Yang, Y.T., Bor, H.Y., Wei, C.N., and Tai, C.C. (2009). Aging effects on the microstructure and creep behavior of Inconel 718 superalloy. Materials Science and Engineering, pp. 289-294.

Li, L. et al. (2015). Machining characteristics of Inconel 718 by sinking-EDM and wire-EDM. Materials and Manufacturing Processes, 30(8): p. 968-973.

Li, X., Shi, J., Cao, G., Russell, A., Zhou, Z., Li, C., and Chen, G. (2019). Improved plasticity of Inconel 718 superalloy fabricated by selective laser melting through a novel heat treatment process, Materials & Design, Volume 180.

Li, X., Shi, J., Wang, C., Cao, G., Russell, A., Zho, Z., Chen, G. (2018). Effect of heat treatment on microstructure evolution of Inconel 718 alloy fabricated by selective laser melting, J. Alloy. Compd. 764 (2018) 639–649.

Liverani, E. et al. (2017). Effect of selective laser melting (SLM) process parameters on microstructure and mechanical properties of 316L austenitic stainless steel. Journal of Materials Processing Technology. 249: p. 255-263.

Long, H. et al. (2018). Microstructural and compositional design of Ni-based single crystalline superalloys—a review. Journal of Alloys and Compounds. 743: p. 203-220.

Lu, Y. et al. (2015). Study on the microstructure, mechanical property and residual stress of SLM Inconel-718 alloy manufactured by differing island scanning strategy. Optics and Laser Technology. 75: p. 197-206.

MatWeb. (2023). MatWeb. Retrieved from MatWeb: https://www.matweb.com/ [accessed: 31.01.2024].

Metals Handbook Volume 9. (2004). Metallography and Microstructures of Heat Resisting Alloys. USA.

Mouritz, A. (2012). Introduction to aerospace materials: Elsevier.

Nicel Institute. (2021). High-temperature high-strength nickel-base alloys no. 393. Nicel Institute. https://nickelinstitute.org/media/8d93486143182f5/nickel_incopub393_updated-june-2021.pdf [accessed: 13.01.2024].

Özsolak, O. (2019). Eklemeli İmalat Yöntemleri ve Kullanılan Malzemeler. International Journal of Innovative Engineering Applications, 3(1), 9-14.

Özsoy, K., and Duman, B. (2017). Eklemeli İmalat (3 Boyutlu Baski) Teknolojilerinin Eğitimde Kullanilabilirliği. International Journal of 3D Printing Technologies and Digital Industry, 1(1), 36-48.

Peng , J., Lv, X., and Lu, Z. (2023). Investigations of the mechanical and high-temperature tribological properties of the Inconel 718 alloy formed by selective laser melting. Tribol Int;188:108813.

Popovich, V., Borisov, E., Popovich, A., Sufiiarov, V., Masaylo, D., and Alzina, L. (2017). Impact of heat treatment on mechanical behaviour of Inconel 718 processed with tailored microstructure by selective laser melting,. Materials & Design, Volume 131,, pp. 12-22.

Poyraz, Ö., and Kuşhan, M. C. (2018). Havacılık Komponentlerinin Bakım Uygulamalarında Katmanlı İmalat Teknolojilerinin Kullanımı. Mühendis Ve Makina, 59(691), 59-69.

Priminox. (2023). The Advantages and Applications of Inconel Flanges. Retrieved from Prinminox Oversizes: https://www.priminox.com/blog/the-advantages-and-applications-of-inconel-flanges/ [accessed: 21.12.2023].

Radavich, J. (1989). The Physical Metallurgy of Cast and Wrought Alloy 718, Superalloy 718-Metallurgy and Applications, Edited by E.A.Loria, P 229-240.

Raghavan, S. et al. (2017). Effect of different heat treatments on the microstructure and mechanical properties in selective laser melted inconel 718 alloy. Materials and Manufacturing Processes. 32(14).

Razavykia, A., Brusa, E., Delprete, C., and Yavari, R. (2020). An Overview of Additive Manufacturing Technologies—A Review to Technical Synthesis in Numerical Study of Selective Laser Melting. Materials, 13.

Reed, R. (2006). The Superalloys: Fundamentals and Applications. Cambridge: Cambridge University Press.

Reed, R. (2008). The Superalloys, Fundamentals and Applications. Cambridge University Press.

Sims, C. (1984). A history of superalloy metallurgy for superalloy metallurgists. Superalloys: p. 399-419.

Sims, T.C., Stoloff, S.N. , and Hagel, C.W. (1987). Superalloys II. John Wiley & Sons.

Slama C., and Abdellaoui M. (2000). Structural characterization of the aged Inconel 718. Journal of Alloys and Compounds,, pp. 277-284.

Sunay, N., Mert, K., and Kaynak, Y. (2020). Chemical Post-Processing Methods For Enhancing Surface Properties Of Parts Fabricated By Additive Manufacturing: A Review. Sigma Journal Of Engineering And Natural Sciences. 38(4): p. 2027-2042.

Thomas, A. et al. (2006). High temperature deformation of Inconel 718. Journal of materials processing technology. 177(1-3): p. 469-472.

Trosch, T. et al. (2016). Microstructure and mechanical properties of selective laser melted Inconel 718 compared to forging and casting. Materials letters. 164: p. 428-431.

Tucho, W.M. et al. (2017). Microstructure and hardness studies of Inconel 718 manufactured by selective laser melting before and after solution heat treatment. Materials Science and Engineering: A. 689: p. 220-232.

Wang, X., and Chou, K. (2019). The effects of stress relieving heat treatment on the microstructure and residual stress of Inconel 718 fabricated by laser metal powder bed fusion additive manufacturing process. Journal of Manufacturing Processes. 48.

Warbuton, P. (1967). Problems of Machining Nickel-Based Alloys. Iron and Steel Institute,. Special Report 94, pp. 151-160.

Xu, L., Cha, Z., Peng, B., Zhou, W., and Chen, X. (2023). Effect of heat treatment on microstructures and mechanical properties of Inconel 718 additively manufactured using gradient laser power, Materials Science and Engineering.

Yalçın, B., and Ergene, B. (2017). Endüstride yeni eğilim olan 3-d eklemeli imalat yöntemive metalurjisi. Uluslararası Teknolojik Bilimler Dergisi, 9(3), 65-88.

Yan, C., Jiang, P., Jia, X., and Wang , X. (2020). 3D printing of bioinspired textured surfaces with superamphiphobicity. Nanoscale 12, 2924–2938. doi: 10.1039/C9NR09620E.

Yizeng Pipe. (2023). Inconel Alloy Pipe Fittings. Retrieved from Yizeng Pipe: https://www.yizengpipe.com/pipe-fitting/inconel-alloy-pipe-fittings.html [accessed: 10.01.2024].

Zhang, D., Niu, W., Cao, X., and Liu, Z. (2015). Effect of standard heat treatment on the microstructure and mechanical properties of selective laser melting manufactured Inconel 718 superalloy, Materials Science and Engineering: A, Volume 644, p. 32-40.

Zhao, Y., Hao, L., and Xiong, W. (2020). Phase transformations during continuous cooling in Inconel 718 alloys manufactured by laser powder bed fusion and suction casting. 2006.01737.

Zhou, J. et al. (2012). Study of surface quality in high speed turning of Inconel 718 with uncoated and coated CBN tools. The International Journal of Advanced Manufacturing Technology 58(1-4): p. 141-151.

Zhou, L., Mehta, A., McWilliams, B., Cho, K., and Sohna, Y. (2019). Microstructure, precipitates and mechanical properties of powder bedfused inconel 718 before and after heat treatmentLe. Journal of Materials Science & Technology 35, 1153–1164.

CURRICULUM VITAE

Can DOĞAN, He spent his childhood in Istanbul and Ankara. He graduated from Ankara Atatürk High School in 2013 and in the same year he enrolled in Çukurova University Mechanical Engineering Department. In 2019, he graduated with a bachelor's degree in mechanical engineering. After completing his military service, he started his master's degree in Mechanical Engineering at Çukurova University. He is currently working as a mechanical maintenance engineer at Bilgin Energy Samsun CCPP.